DOE Review Release 09/26/2024

Uncertainty in Fitted Dose in Internal Dose Assessments

ORAUT-RPRT-0109 Rev. 00
Effective Date: 09/20/2024
Supersedes: None

Subject Expert(s): Thomas R. LaBone, Elizabeth M. Brackett, and Mutty M. Sharfi

Document Owner Approval:	Signature on File Nancy Chalmers, Document Owner	Approval Date:	09/18/2024
Concurrence:	Signature on File Wade C. Morris, Objective 1 Manager	Concurrence Date:	09/18/2024
Concurrence:	Signature on File Scott R. Siebert, Objective 3 Manager	Concurrence Date:	09/19/2024
Concurrence:	Signature on File Jennifer L. Hoff, Acting Project Director	Concurrence Date:	09/18/2024
Approval:	Signature on File Timothy D. Taulbee, Associate Director for Science	Approval Date:	09/20/2024

**FOR DOCUMENTS MARKED AS A TOTAL REWRITE OR REVISION,
REPLACE THE PRIOR REVISION AND DISCARD / DESTROY ALL COPIES OF THE PRIOR REVISION.**

☒ New ☐ Total Rewrite ☐ Revision

PUBLICATION RECORD

EFFECTIVE DATE	REVISION NUMBER	DESCRIPTION
09/20/2024	00	New report justifying the use of a geometric standard deviation of 3 when quantifying the uncertainty in fitted dose. Incorporates formal internal and NIOSH review comments. Training is not required. Initiated by John M. Byrne and authored by Nancy Chalmers.

TABLE OF CONTENTS

LIST OF TABLES

LIST OF FIGURES

ACRONYMS AND ABBREVIATIONS

AMAD	activity median aerodynamic diameter
Bq	becquerel
d	day
DCF	dose conversion factor
DOE	U.S. Department of Energy
dpm	disintegrations per minute
F	fast (absorption type)
FGR-13	Federal Guidance Report 13
g	gram
GM	geometric mean
GSD	geometric standard deviation
HTO	tritiated water
ICRP	International Commission on Radiological Protection
IREP	Interactive RadioEpidemiological Program
IRF	intake retention fraction
MBq	megabecquerel
MeV	megaelectron-volt (1 million electron-volts)
nCi	nanocurie
NCRP	National Council on Radiation Protection and Measurements
NIOSH	National Institute for Occupational Safety and Health
ORAU	Oak Ridge Associated Universities
ORAUT	ORAU Team
pCi	picocurie
S	slow (absorption type)
SRDB Ref ID	Site Research Database Reference Identification (number)
V	vapor (absorption type)
µCi	microcurie
µm	micrometer
µSv	microsievert

1.0 INTRODUCTION

The Oak Ridge Associated Universities (ORAU) Team uses the Interactive RadioEpidemiological Program (IREP) to calculate probability of causation for cancer in a specified organ as a function of dose to that organ over time. The organ dose is assigned annually as a probability distribution, which can be a constant. ORAUT-OTIB-0060, *Internal Dose Reconstruction*, assumes that the uncertainty associated with fitted doses[1] comes from the "uncertainty in the bioassay measurements and the biokinetic models" [ORAU Team (ORAUT) 2018, p. 18]. When the dose is lognormally distributed, it is assumed to have a geometric standard deviation (GSD) of 3. The justification for the GSD of 3 was apparently discussed early in the history of the dose reconstruction project, but the only documentation is in Brackett et al. [2008, p. 9] and Boecker et al. [1991, pp. 33, 62]. The purpose of this report is to provide technical justification for a GSD of 3 for fitted dose.

This report splits the total uncertainty in fitted organ dose into (1) uncertainty in the biokinetic/dosimetric models (i.e., in the dose conversion factors [DCFs]) and (2) uncertainty in the fitted intakes. The uncertainty in the DCFs is discussed in Section 2.0, and the uncertainty in fitted intakes is discussed in Section 3.0. Section 4.0 shows how the uncertainties from these two sources are propagated to give the total fitted organ dose uncertainty. Attachment A discusses uncertainty in estimated intakes, and Attachment B explains the bias-variance tradeoff in uncertainty. Attachment C contains extended descriptions of figures. ORAUT [2024] contains the analysis calculations.

2.0 UNCERTAINTY FROM DOSE CONVERSION FACTORS

Section 2.1 discusses a report on the uncertainties in Federal Guidance Report 13, *Cancer Risk Coefficients for Environmental Exposure to Radionuclides* cancer risk estimates [FGR-13; Eckerman et al. 1999]. Section 2.2 compares these uncertainties with those of the committed organ DCF analysis in National Council on Radiation Protection and Measurements (NCRP) Report No. 164, *Uncertainties in Internal Radiation Dose Assessment* [NCRP 2009].

2.1 FEDERAL GUIDANCE REPORT 13

FGR-13 gives cancer risk estimates for the inhalation[2] of approximately 2,300 different radioactive materials (combinations of radionuclides and absorption types) by members of the public. An Oak Ridge National Laboratory report, *Uncertainties in Cancer Risk Coefficients for Environmental Exposure to Radionuclides*, discusses the uncertainties in these risk estimates [Pawel et al. 2007]. The range of cancer risk estimates in Table D-2 of Pawel et al. is the basis for deriving values for the uncertainty in DCFs. The uncertainties in Pawel et al. include cancer risk, so the cancer risk uncertainties need to be stripped out so that only the uncertainties in the DCFs remain.

The uncertainties in Pawel et al. [2007] are expressed as the ratio of 95th and 5th percentiles (Q_{95} and Q_5, respectively). Each material considered in the report was placed into one of five categories by the authors, where Category A was the least uncertain and Category E was the most uncertain (see the first and second columns of Table 2-1).

---

1 Fitted doses are calculated from intakes that are based on positive bioassay results.

2 All particulates are assumed to have known solubility and an activity median aerodynamic diameter (AMAD) of 1 μm. Risk can change due to AMAD, but the uncertainty in risk likely will not. Uncertainties for 1-μm AMAD can reasonably be applied to 5-μm AMAD aerosols.

Table 2-1. Summary of uncertainties derived from the analysis in Pawel et al. [2007].[a]

Category	Definition	GSD (includes cancer risk)	GSD_{DCF} (excludes cancer risk)[b]
A	$Q_{95}/Q_5 < 15$	GSD < 2.278	$GSD_{DCF} < 1.570$
B	$15 \le Q_{95}/Q_5 < 35$	2.278 ≤ GSD < 2.947	$1.570 \le GSD_{DCF} < 1.808$
C	$35 \le Q_{95}/Q_5 < 65$	2.947 ≤ GSD < 3.557	$1.808 \le GSD_{DCF} < 2.004$
D	$65 \le Q_{95}/Q_5 < 150$	3.557 ≤ GSD < 4.586	$2.004 \le GSD_{DCF} < 2.303$
E	$Q_{95}/Q_5 \ge 150$	GSD ≥ 4.586	$GSD_{DCF} \ge 2.303$

a. Source: Pawel et al. [2007].
b. GSD_{DCF} = the uncertainty in the DCFs; see Equations 2-5 to 2-7.

Assuming a lognormal distribution:

$$\frac{Q_{95}}{Q_5} = \frac{GM \times GSD^{1.645}}{GM \times GSD^{-1.645}} = GSD^{3.290} \tag{2-1}$$

where

GM = geometric mean
GSD = geometric standard deviation
1.645 = the 95th percentile of a standard normal distribution

Therefore, the GSD is:

$$GSD = \left(\frac{Q_{95}}{Q_5} \right)^{1/3.290} \tag{2-2}$$

For example, for Category A materials:

$$\frac{Q_{95}}{Q_5} < 15 \tag{2-3}$$

$$GSD < (15)^{1/3.290} = 2.278 \tag{2-4}$$

The GSD (including cancer risk) for each category is in the third column of Table 2-1.

Pawel et al. [2007] decomposed the cancer risk uncertainties for 15 different materials into (1) the uncertainty in cancer risk models and (2) the uncertainty in the DCFs (see Table 2-2).

Table 2-2. Summary of Table 6 in Pawel et al. [2007].[a,b]

Intake	Relative uncertainty cancer model (%) / DCFs (%)[c]
Ingestion HTO	80/20
Inhalation HTO	80/20
Ingestion Co-60	70/30
Inhalation Co-60	70/30
Ingestion Sr-90	65/35
Inhalation Zr-95	85/15
Ingestion Ru-106	95/5
Ingestion I-131	95/5
Ingestion Cs-137	85/15
Inhalation Cs-137	85/15
Ingestion Gd-148	80/20
Ingestion Ra-226	90/10
Ingestion U-234	90/10
Inhalation U-234	80/20
Inhalation Pu-238	98/2

a. Source: Pawel et al. [2007].
b. HTO = tritiated water.
c. The ratio in the third column is the percent of total uncertainty attributed to the cancer risk model over the percent of total uncertainty attributed to the DCFs.

Based on Table 2-2, assume that a 70/30 partition of uncertainty is reasonable for all materials, where 70% of the uncertainty comes from the cancer risk model and 30% from the DCFs. Assuming the uncertainty in the cancer risk model is independent of the uncertainty in the DCFs:

$$\left(\log GSD_{\text{DCF}}\right)^2 = 0.3 \times \left(\log GSD\right)^2 \tag{2-5}$$

$$GSD_{\text{DCF}} = \exp\left(\sqrt{0.3 \times \left(\log GSD\right)^2}\right) \tag{2-6}$$

where

GSD_{DCF} = the uncertainty in the DCFs and “log” refers to the natural logarithm

Therefore, for Category A:

$$GSD_{\text{DCF}} < \exp\left(\sqrt{0.3 \times \left(\log 2.278\right)^2}\right) = 1.570 \tag{2-7}$$

The uncertainty in the DCFs (GSD_{DCF}) is given in the fourth column of Table 2-1. Note that Category E has few materials of practical interest (see Figure 2-1 and Table 2-3).

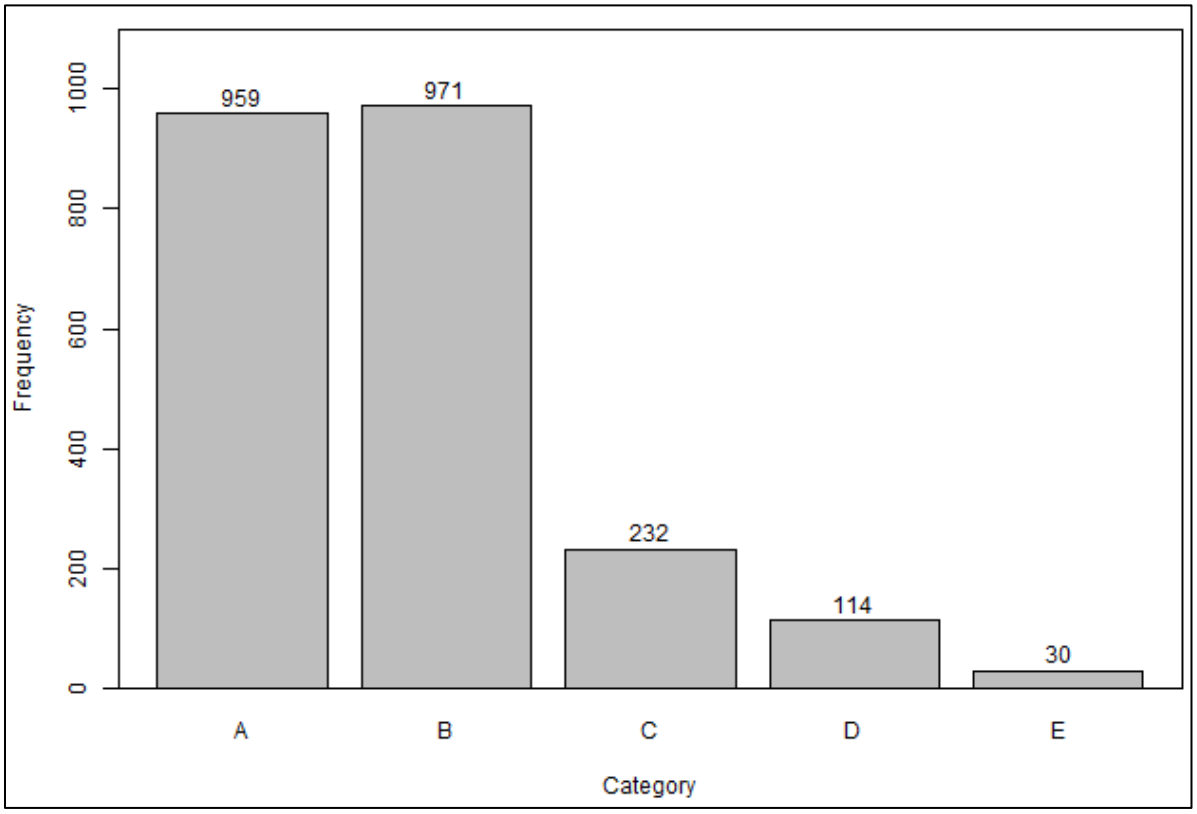

Figure 2-1. Summary of the number of radioactive materials (combinations of radionuclides and absorption types) in each uncertainty category.

Table 2-3. Category E materials.[a,b]

Nuclide	Type
Si-32	F
Te-123	V
W-178	F
W-185	F
Pb-212	F
Pa-230	F
U-230	F
S-35	F
Os-191	F
Os-194	F

Nuclide	Type
Bi-210	F
Bi-210m	F
At-211	F
U-237	F
Cf-246	F
Te-123	F
Fr-223	F
Ra-223	F
Ra-224	F
Ra-225	F

Nuclide	Type
Ra-226	F
Ac-224	F
Ac-225	F
Ac-226	F
Th-227	F
Es-253	F
Es-254m	F
Fm-252	F
Fm-253	F
Fm-255	F

a. Source: Pawel et al. [2007].
b. V = vapor.

2.2 NCRP REPORT NO. 164

Table 2-4 summarizes the uncertainties in the committed organ DCFs for 20 different cases in NCRP Report No. 164, which are expressed as the ratio of the upper bound to the lower bound. The NCRP values for effective dose are not included in Table 2-4 because this analysis concerns only organ DCFs.

Table 2-4. Summary of Table 9.1 in NCRP Report No. 164.[a]

Case	Nuclide	Pathway	Pattern	Organ	Form	Ratio	GSD
1	C-14	Inhalation	Chronic	Bone marrow	Known	50.0	2.32
2	Sr-90	Ingestion	Chronic	Bone surfaces	Known	17.0	1.84
2	Sr-90	Ingestion	Chronic	Bone marrow	Known	12.0	1.71

Case	Nuclide	Pathway	Pattern	Organ	Form	Ratio	GSD
3	Sr-90	Inhalation	Chronic	Lung	Known	10.0	1.64
3	Sr-90	Inhalation	Chronic	Bone surfaces	Known	20.0	1.90
3	Sr-90	Inhalation	Chronic	Bone marrow	Known	14.0	1.76
4	U-238	Inhalation	Acute	Lung	Unknown	600.0	3.95
4	U-238	Inhalation	Acute	Colon	Unknown	15.0	1.79
4	U-238	Inhalation	Acute	Bone marrow	Unknown	100.0	2.69
4	U-238	Inhalation	Acute	Kidney	Unknown	100.0	2.69
5	Sr-90	Inhalation	Acute	Lung	Unknown	6,000.0	6.49
5	Sr-90	Inhalation	Acute	Bone surfaces	Unknown	150.0	2.94
5	Sr-90	Inhalation	Acute	Bone marrow	Unknown	150.0	2.94
6	I-131	Ingestion	Acute	Thyroid	Known	5.4	1.44
7	I-131	Ingestion	Chronic	Thyroid	Known	3.4	1.30
8	I-131	Inhalation	Chronic	Thyroid	Known	3.6	1.32
8	I-131	Inhalation	Chronic	Thyroid	Known	3.6	1.32
8	I-131	Inhalation	Chronic	Thyroid	Known	4.0	1.35
8	I-131	Inhalation	Chronic	Thyroid	Known	4.0	1.35
8	I-131	Inhalation	Chronic	Thyroid	Known	6.0	1.47
8	I-131	Inhalation	Chronic	Thyroid	Known	7.0	1.52
9	Cs-137	Ingestion	Acute	Colon	Known	5.0	1.41
9	Cs-137	Ingestion	Acute	Bone marrow	Known	2.0	1.16
10	Cs-137	Ingestion	Acute	Colon	Unknown	5.0	1.41
10	Cs-137	Ingestion	Acute	Bone marrow	Unknown	160.0	2.98
11	Cs-137	Inhalation	Acute	Lung	Known	10.0	1.64
11	Cs-137	Inhalation	Acute	Colon	Known	3.5	1.31
11	Cs-137	Inhalation	Acute	Bone marrow	Known	3.5	1.31
12	Cs-137	Inhalation	Acute	Lung	Unknown	60.0	2.41
12	Cs-137	Inhalation	Acute	Colon	Unknown	10.0	1.64
12	Cs-137	Inhalation	Acute	Bone marrow	Unknown	10.0	1.64
13	Ru-106	Ingestion	Acute	Colon	Known	25.0	2.00
13	Ru-106	Ingestion	Acute	Kidney	Known	40.0	2.21
13	Ru-106	Ingestion	Acute	liver	Known	36.0	2.16
13	Ru-106	Ingestion	Acute	Bone marrow	Known	25.0	2.00
14	U-238	Inhalation	Acute	Lung	Known	75.0	2.53
14	U-238	Inhalation	Acute	Colon	Known	20.0	1.90
14	U-238	Inhalation	Acute	Bone marrow	Known	50.0	2.32
14	U-238	Inhalation	Acute	Kidney	Known	25.0	2.00
15[b]	U-238	Inhalation	Acute	Lung	Unknown	600.0	3.95
15[b]	U-238	Inhalation	Acute	Colon	Unknown	15.0	1.79
15[b]	U-238	Inhalation	Acute	Bone marrow	Unknown	100.0	2.69
15[b]	U-238	Inhalation	Acute	Kidney	Unknown	100.0	2.69
16[b]	U-238	Inhalation	Acute	Lung	Unknown	600.0	3.95
16[b]	U-238	Inhalation	Acute	Colon	Unknown	15.0	1.79
16[b]	U-238	Inhalation	Acute	Bone marrow	Unknown	100.0	2.69
16[b]	U-238	Inhalation	Acute	Kidney	Unknown	100.0	2.69
17	Pu-239	Inhalation	Acute	Lung	Known	20.0	1.90
17	Pu-239	Inhalation	Acute	Colon	Known	100.0	2.69
17	Pu-239	Inhalation	Acute	Bone marrow	Known	50.0	2.32
18	Pu-239	Inhalation	Acute	Lung	Unknown	100.0	2.69
18	Pu-239	Inhalation	Acute	Colon	Unknown	150.0	2.94
18	Pu-239	Inhalation	Acute	Bone marrow	Unknown	150.0	2.94
19	Cf-252	Inhalation	Acute	Lung	Known	10.0	1.64
19	Cf-252	Inhalation	Acute	Colon	Known	150.0	2.94
19	Cf-252	Inhalation	Acute	Bone marrow	Known	20.0	1.90
19	Cf-252	Inhalation	Acute	Bone surfaces	Known	20.0	1.90
20	Cf-252	Inhalation	Acute	Lung	Unknown	200.0	3.12

Case	Nuclide	Pathway	Pattern	Organ	Form	Ratio	GSD
20	Cf-252	Inhalation	Acute	Colon	Unknown	100.0	2.69
20	Cf-252	Inhalation	Acute	Bone marrow	Unknown	400.0	3.62
20	Cf-252	Inhalation	Acute	Bone surfaces	Unknown	400.0	3.62

a. Source: NCRP [2009].
b. Cases 15 and 16 are duplicates of Case 4 in the NCRP document. This analysis does not use any of them because the form is unknown.

The NCRP considered these upper and lower bounds to represent a likely range based on current information but did not attribute any particular probability to them. Assuming the 99th and 1st percentiles (Q_{99} and Q_1, respectively) of a lognormal distribution are the upper bound and lower bound, respectively:

$$\frac{Q_{99}}{Q_1} = \frac{GM \times GSD^{2.326}}{GM \times GSD^{-2.326}} = GSD^{4.653} \tag{2-8}$$

$$GSD = \left(\frac{Q_{99}}{Q_1} \right)^{1/4.653} \tag{2-9}$$

where

Q_{99} = 99th percentile
Q_1 = 1st percentile
2.326 = 99th percentile of a standard normal distribution

Calculated GSDs assuming the 99th and 1st percentiles are in the GSD column of Table 2-4.

Cases where the absorption type (“Form” column in Table 2-4) is unknown are irrelevant to the discussion of uncertainty in DCFs because the uncertainty in the solubility is considered when estimating the uncertainty in the intake, not the uncertainty in the DCF. Therefore, cases with unknown absorption type were excluded. Figure 2-2 is a lognormal probability plot of the 12 relevant cases, where material type is known. The GSDs from NCRP Report No. 164 (excluding those with unknown material type) are consistent[3] with those in FGR-13 from Table 2-1 (after stripping out cancer risk). The category-based uncertainties in DCFs from Table 2-1 are derived from approximately 2,300 different radioactive materials, whereas the uncertainties from Table 2-4 are derived from only 8 nuclides, so the uncertainties in DCFs from Table 2-1 were used for the analysis in Section 4.0.

The GSDs for DCFs derived from FGR-13 are applicable to occupational exposures because the same International Commission on Radiological Protection (ICRP) Publication 68 models are used for occupational and environmental exposures [ICRP 1995]. While the focus of this report is fitted dose, the uncertainties in DCFs in Table 2-1 are applicable for any dose calculations using these DCFs for all organs and all periods.

[3] FGR-13 assumes known absorption types, so stripping cancer risk from the uncertainties in FGR-13 leaves just the uncertainty in DCFs, which is what is used in dose reconstruction. NCRP Report No. 164 does not include cancer risk, but there are cases with unknown material type that must be excluded, to leave just uncertainty in DCFs.

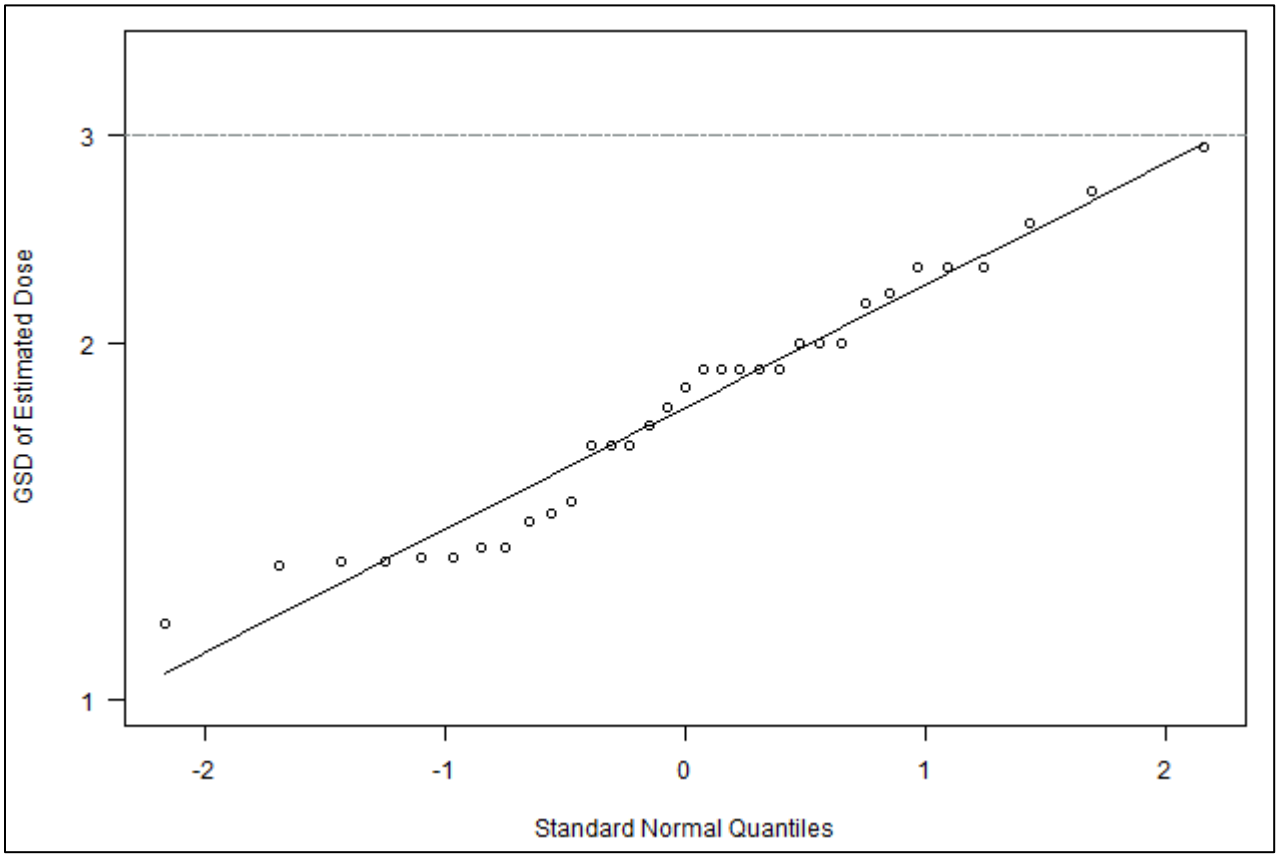

Figure 2-2. Lognormal probability plot of organ dose GSDs calculated from 12 relevant cases in Table 2-4 where the chemical form of the radionuclide was assumed to be known. Attachment C contains an extended description.

3.0 UNCERTAINTY FROM FITTED INTAKES

This section addresses how to calculate the uncertainty in a fitted intake, which is defined as a regression of bioassay data on the intake retention fractions (IRFs) that minimizes (in some sense) the distance between the predictions of the model and the observed data. A fitted intake is a best fit in the statistical meaning of the term (i.e., an unbiased fit). Full-blown uncertainty analyses of every fitted intake used in dose reconstructions are impractical at best because of the complexity of such evaluations. Therefore, some simplifying assumptions are used to facilitate these calculations:

- The uncertainties associated with several well-defined acute[4] intakes of various radionuclides are evaluated to develop a general idea of the range of uncertainties that might be encountered in practice. These uncertainties are generalized and assigned to intakes calculated in a routine dose reconstruction (see Section 3.1).

- The best estimate of an intake is calculated by weighted least squares regression and the uncertainty in the intake is lognormally distributed (see Attachment A).

- When calculating the uncertainty, assume that there are no systematic errors in the biokinetic model (i.e., the right model) and that any random errors in the model are absorbed into the uncertainty in the bioassay data. Uncertainty is thus estimated by looking strictly at how close

[4] The statistical method used to estimate intake uncertainty can be used with any intake pattern if the IRFs are accurately defined.

the predictions of the regression are to the observations (or conversely how much scatter is around the line of best fit).

  - If an intake is calculated from very few data (one or two points), the uncertainty in the intake would tend to be smaller than the uncertainty in the examples in Section 3.1, because fewer data means less scatter around the line of best fit.

  - Urine bioassays for actinides tend to have a lot of scatter around the line of best fit, usually more than any other material. The examples in Section 3.1 include actinides, so the uncertainties in the examples should be bounding.

  - Section 2.2 states that the uncertainty in the solubility is considered when estimating the uncertainty in the intake. For this method of estimating intake uncertainty, the assumption of the right model includes an assumption that the solubility is known. In dose reconstruction, all potential solubility types are considered and the highest is assigned, so the choice of solubility type is not a source of uncertainty (see Attachment B).

- Multiple intakes of a given radionuclide are correlated,[5] and therefore so are the doses they deliver. There is no simple way to account for the correlation in intakes or doses.[6] For this reason, the generalized uncertainty derived for a single intake should be assigned to each of the multiple intakes calculated in a dose reconstruction, and these intakes are assumed to be uncorrelated.

- An intake that is intentionally biased high or low has a smaller uncertainty than the uncertainty in a fitted intake (see Attachment B).

3.1 GENERALIZED UNCERTAINTY IN FITTED INTAKES

Using the methods in Attachment A, the analysis evaluated 10 different acute intakes of 9 radionuclides (tritiated water [HTO], ^{137}Cs, ^{241}Am, ^{144}Ce, ^{99}Mo, ^{239}Pu, enriched uranium, ^{125}I, and ^{35}S). This method calculates n intakes from n bioassay results by regressing each bioassay result on the IRFs. The geometric mean GM_I and geometric standard deviation GSD_I of the n intakes are then calculated. For each of the 10 examples, there are two plots:

1. The first plot is a lognormal probability plot of the individual intake estimates. The purpose of these plots is to show that the distribution of the individual intakes can be reasonably described with a lognormal distribution having the indicated GM_I and GSD_I.

2. The second plot is a scatterplot of the bioassay measurements versus the IRFs. The predicted bioassay measurement is the black line, the slope of which is GM_I. The red dashed lines denote the 95% uncertainty band for the predicted bioassay measurements.

The results of the 10 evaluations are shown in Figures 3-1 to 3-20, and brief details about the cases are presented in the figure captions. The 10 examples include radioactive materials from all the DCF categories in Table 2-1. The values of GSD_I range from just above one to just above two and are summarized in Table 4-1.

[5] The true intakes (or the intake events) are not correlated, but the intakes calculated from correlated bioassay data are.
[6] IREP does not account for correlation among doses.

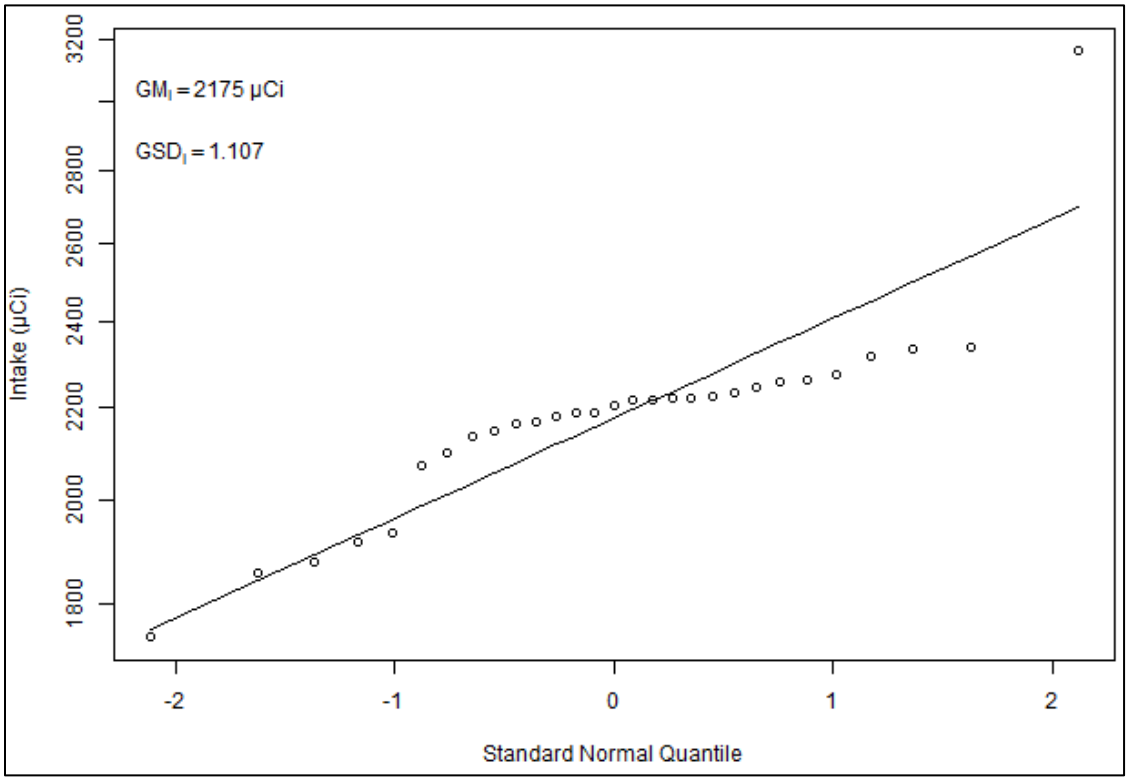

Figure 3-1. Lognormal probability plot of the individual intake estimates from 29 urine bioassays collected after an acute inhalation intake of HTO at Savannah River Site. Attachment C contains an extended description.

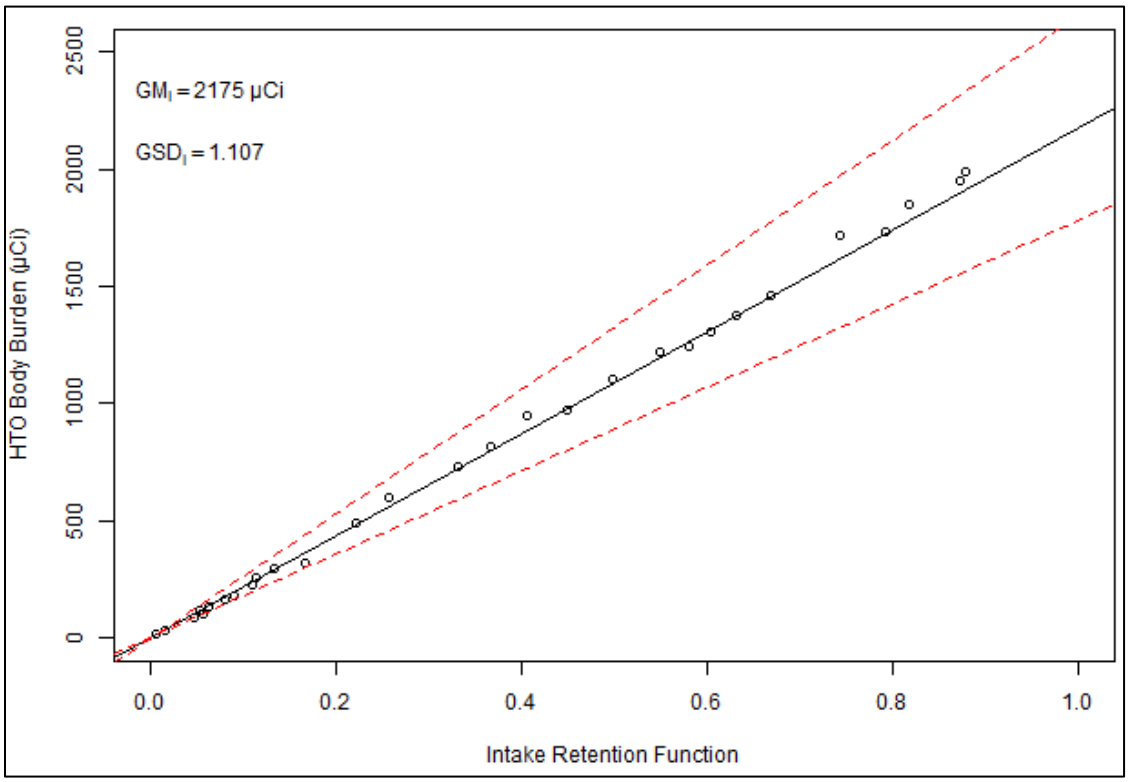

Figure 3-2. Scatterplot of the 29 HTO body burdens versus the IRFs. Attachment C contains an extended description.

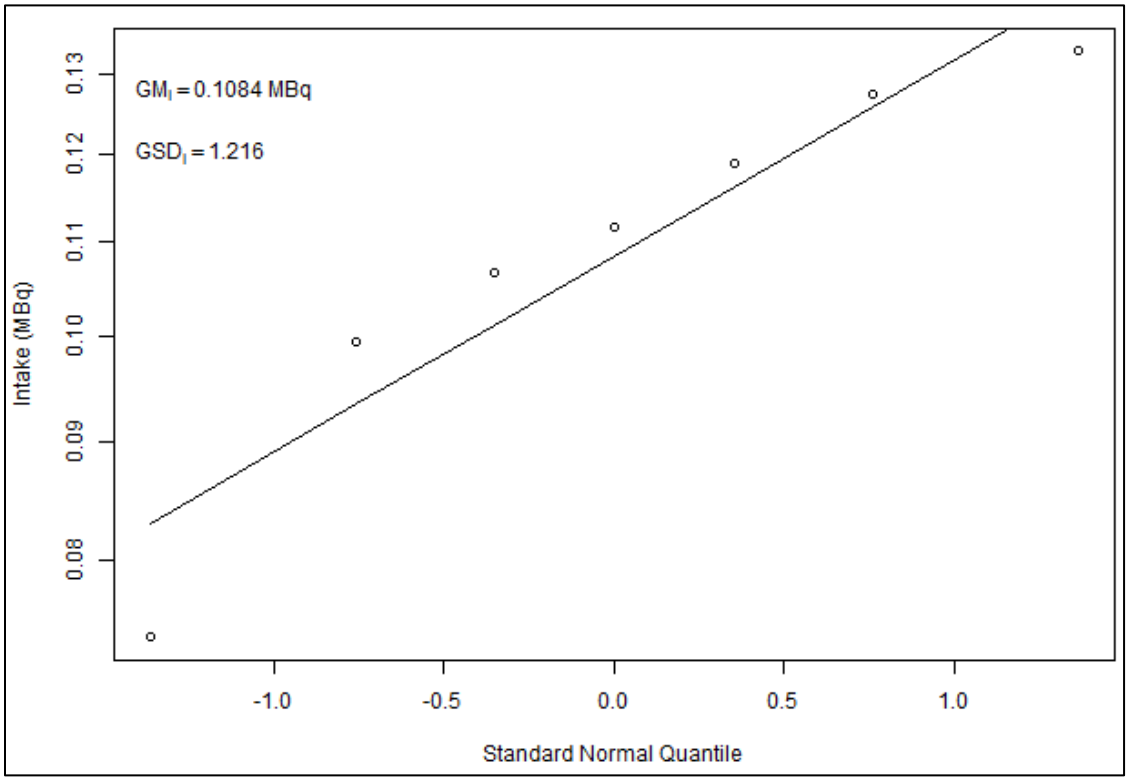

Figure 3-3. Lognormal probability plot of the individual intake estimates from seven whole body counts performed after an acute inhalation intake of ^{137}Cs at a graphite reactor. Attachment C contains an extended description.

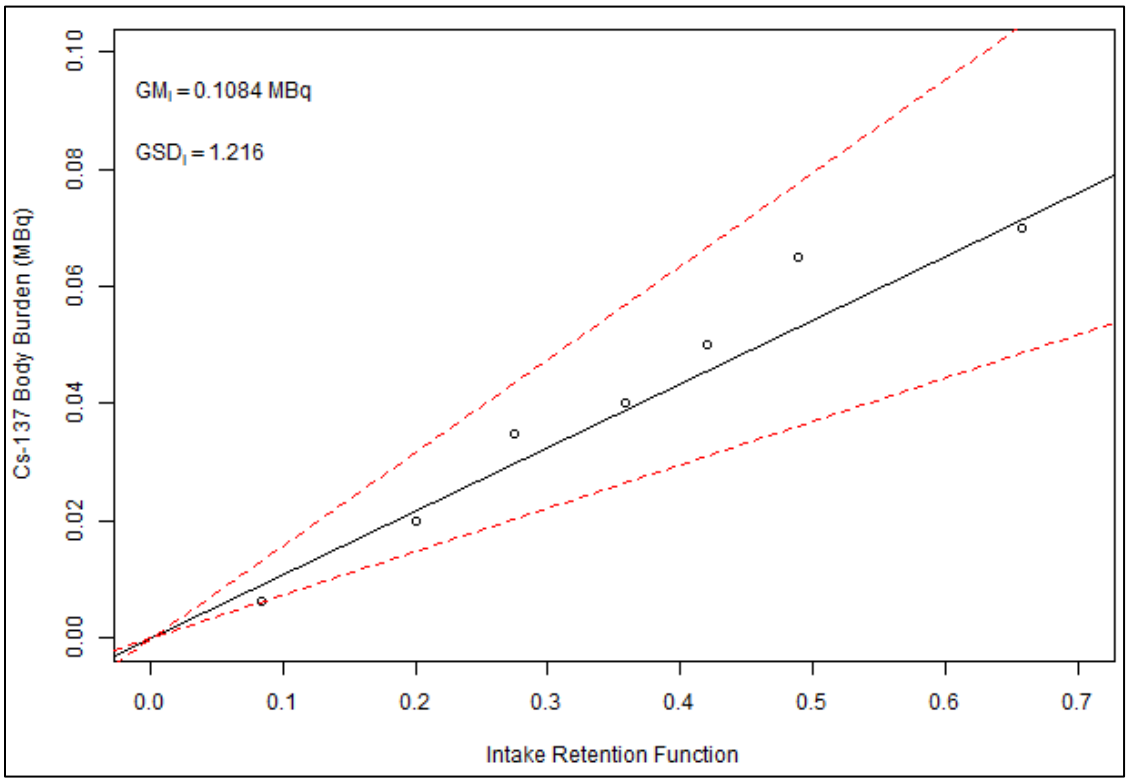

Figure 3-4. Scatterplot of the seven ^{137}Cs body burdens versus the IRFs. Attachment C contains an extended description.

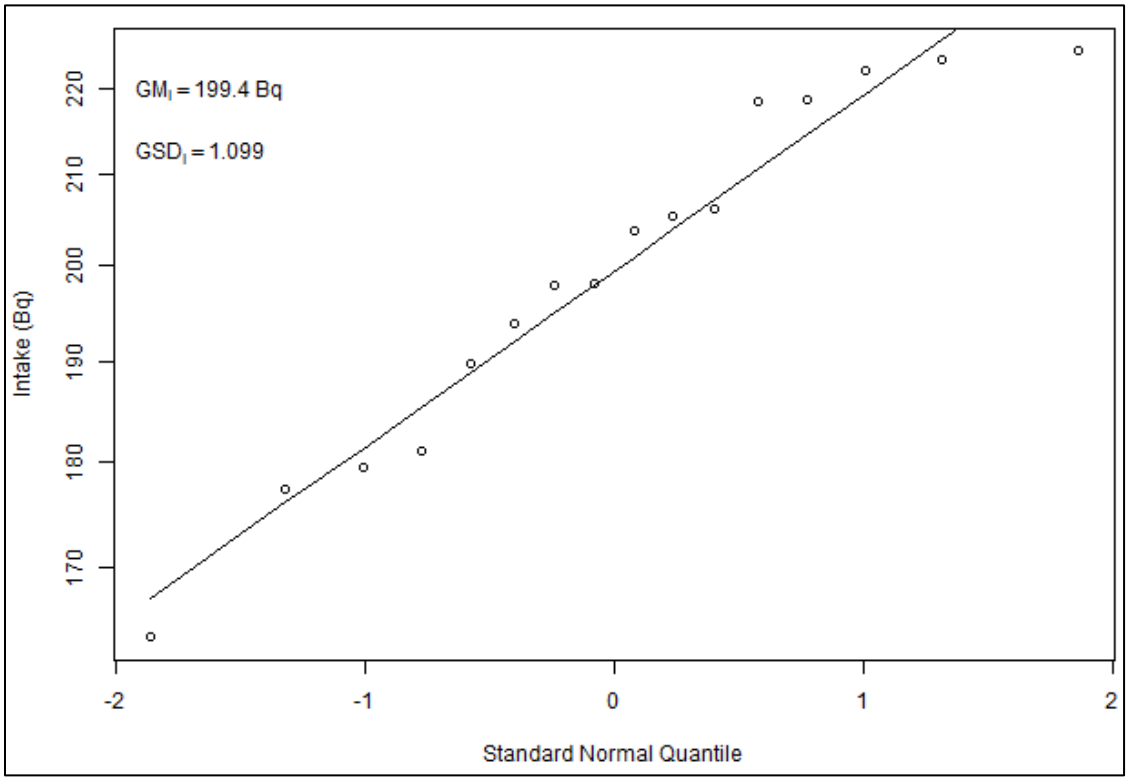

Figure 3-5. Lognormal probability plot of the individual intake estimates from 16 chest counts performed after an acute inhalation intake of Type S ^{241}Am at Savannah River Site. Attachment C contains an extended description.

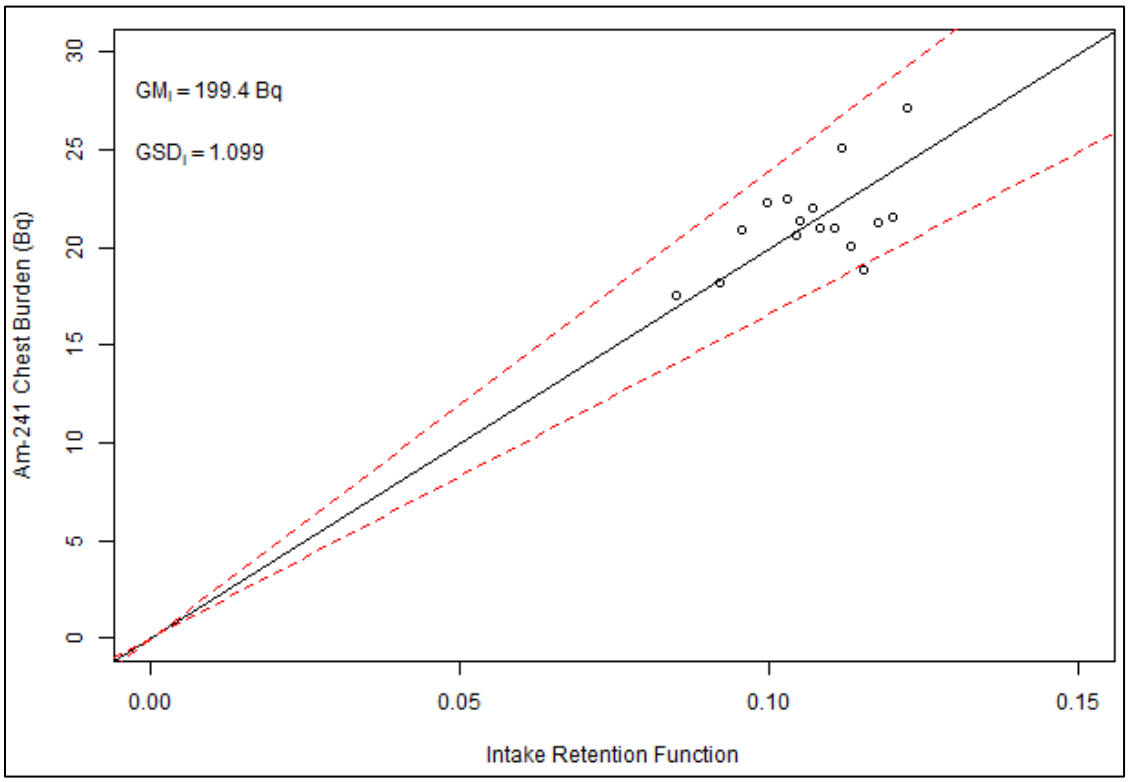

Figure 3-6. Scatterplot of the 16 ^{241}Am chest burdens versus the IRFs. Attachment C contains an extended description.

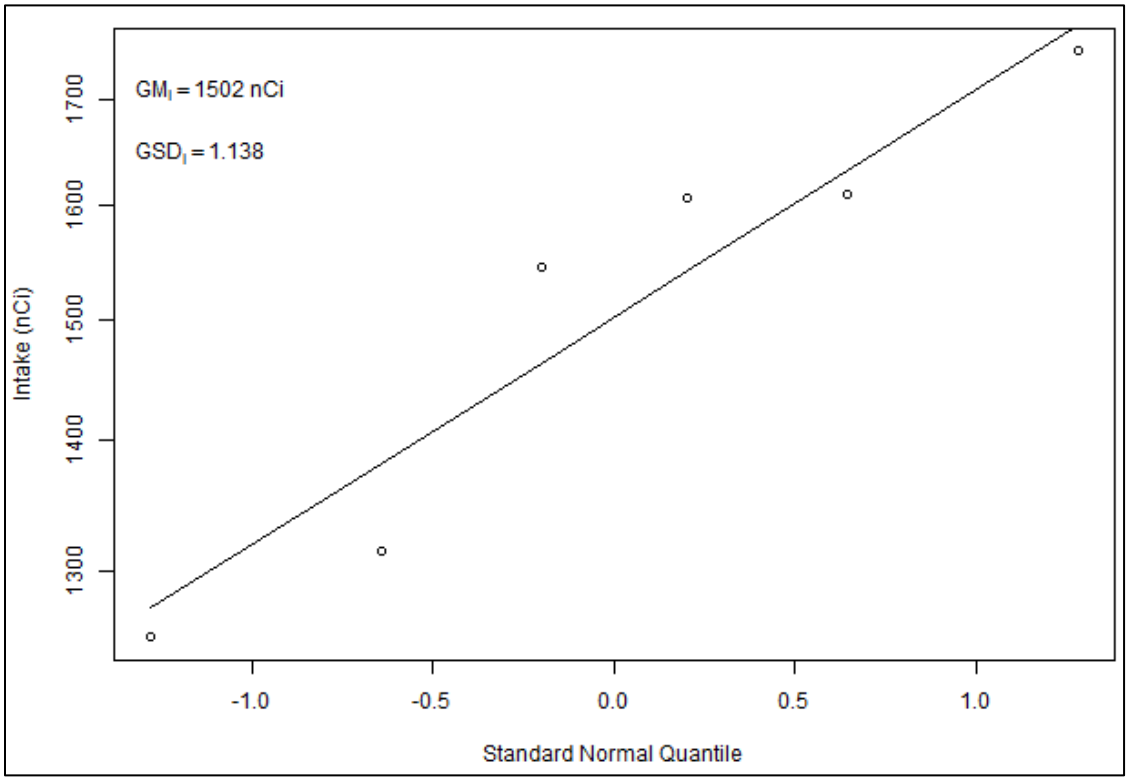

Figure 3-7. Lognormal probability plot of the individual intake estimates from six whole body counts performed after an acute inhalation intake of Type S ^{144}Ce at Savannah River Site. Attachment C contains an extended description.

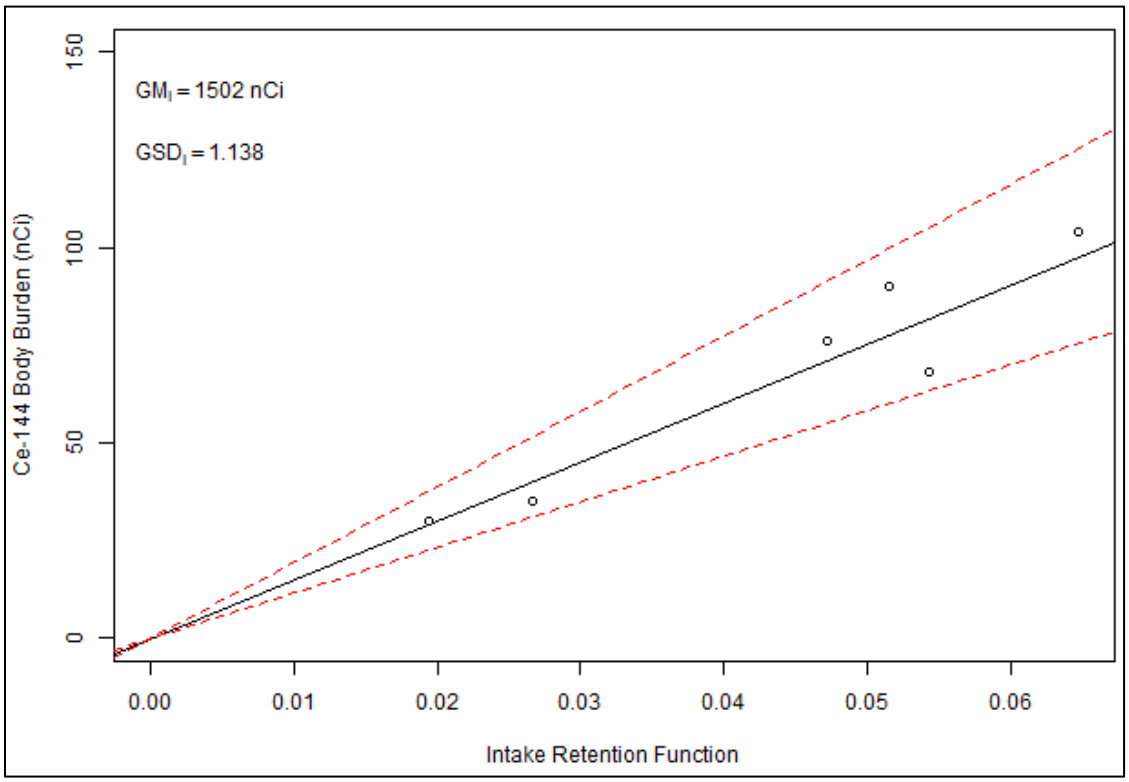

Figure 3-8. Scatterplot of the six ^{144}Ce body burdens versus the IRFs. Attachment C contains an extended description.

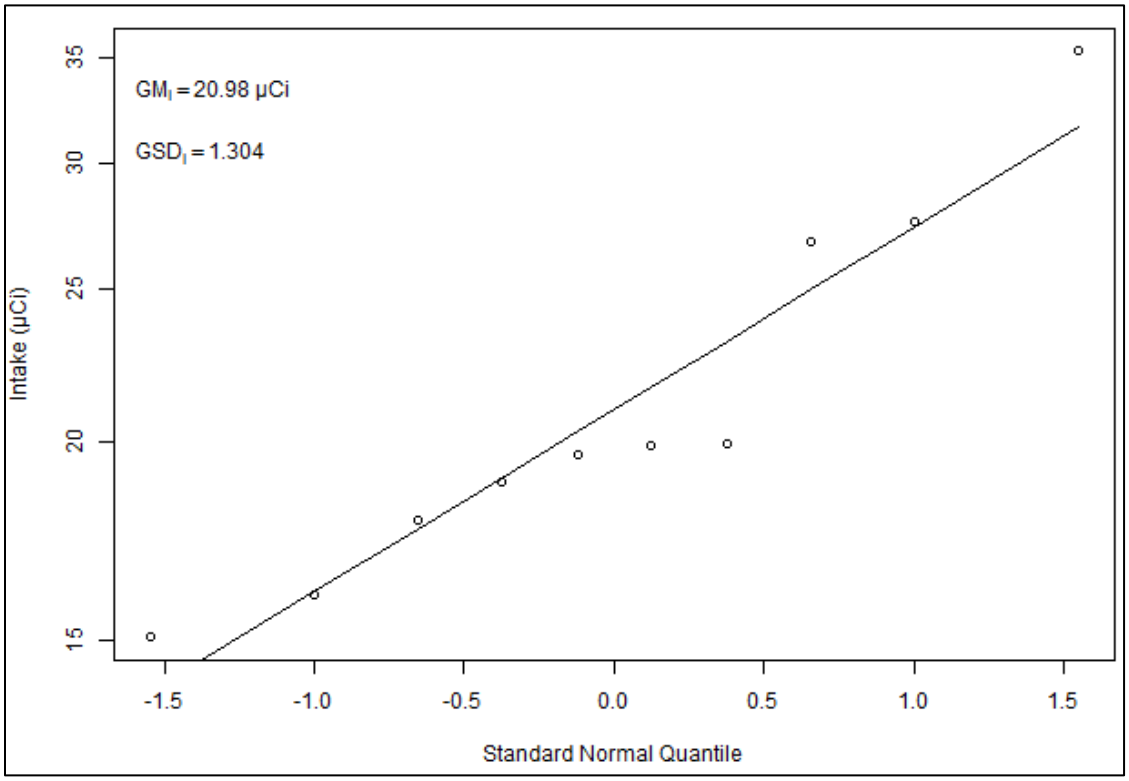

Figure 3-9. Lognormal probability plot of the individual intake estimates from 10 whole body counts performed after an acute inhalation intake of Type F ^{99}Mo at a commercial radiopharmaceutical company. Attachment C contains an extended description.

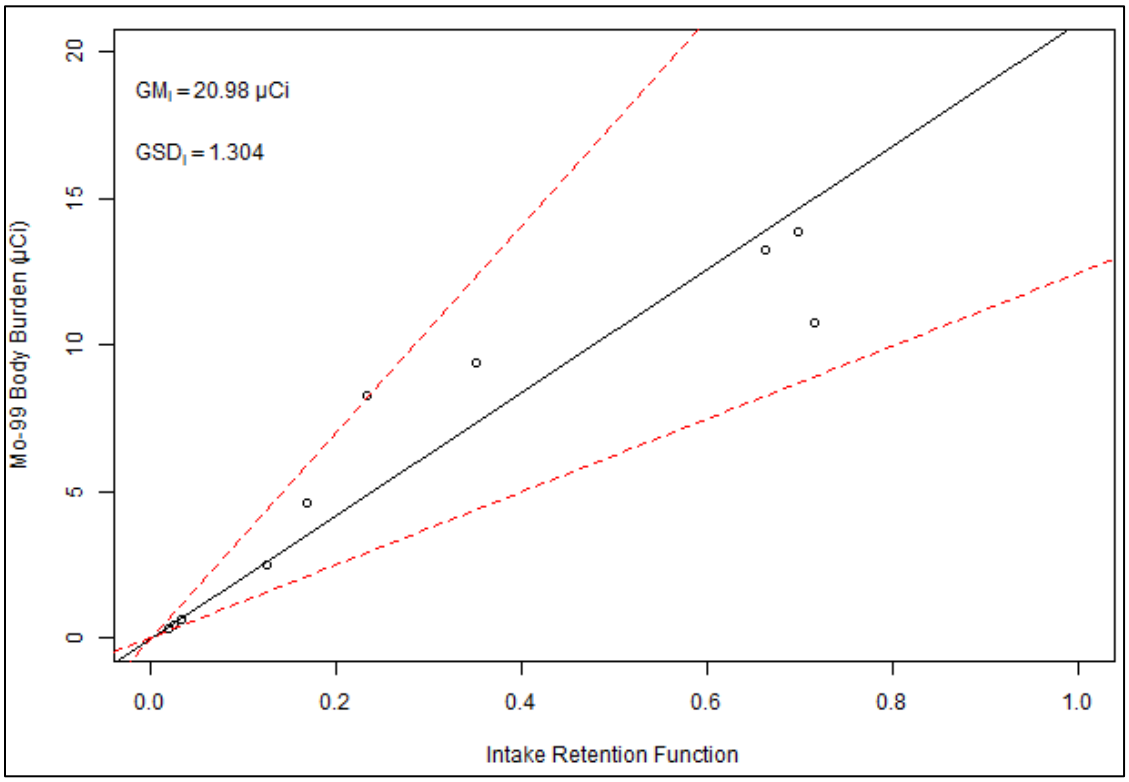

Figure 3-10. Scatterplot of the 10 ^{99}Mo body burdens versus the IRFs. Attachment C contains an extended description.

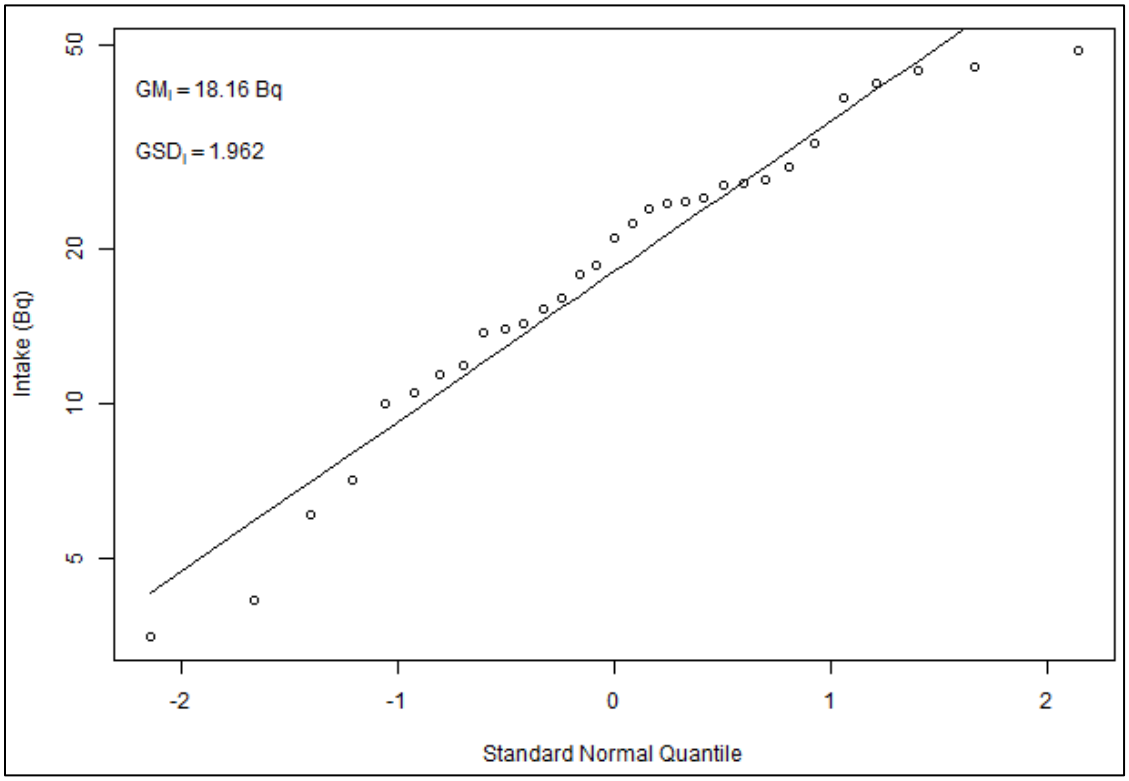

Figure 3-11. Lognormal probability plot of the individual intake estimates from 31 urine bioassays collected after a wound intake of ^{239}Pu at Los Alamos National Laboratory. Attachment C contains an extended description.

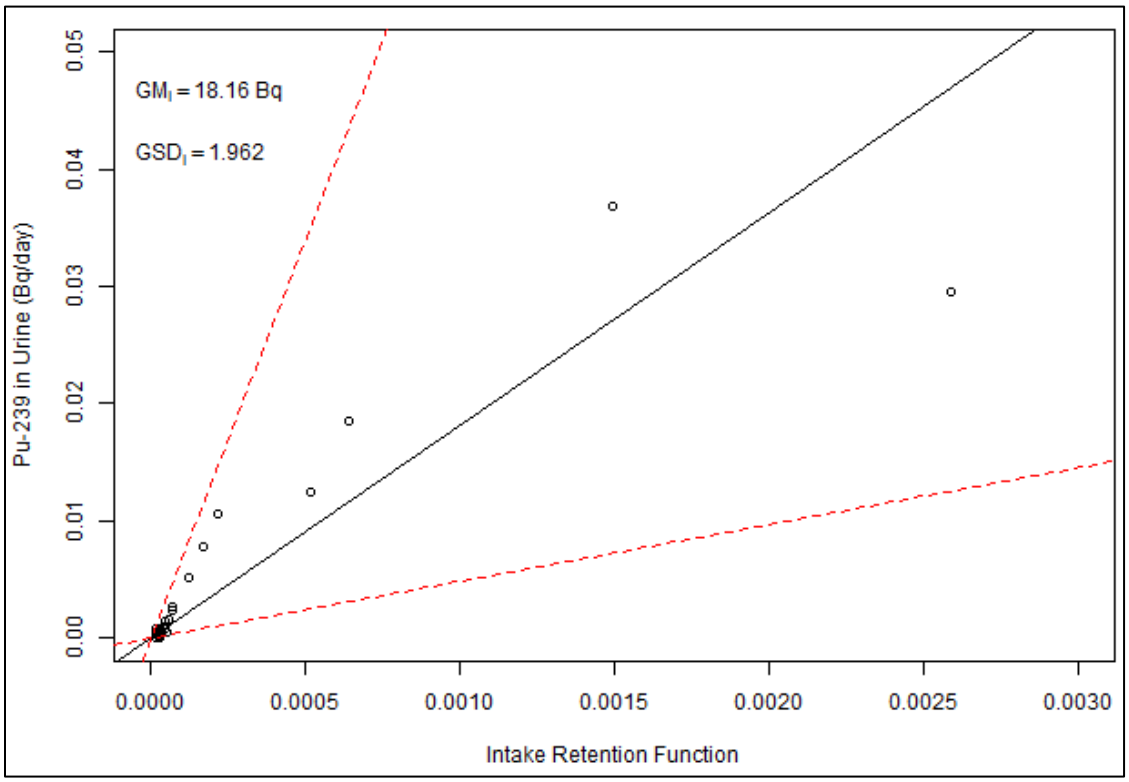

Figure 3-12. Scatterplot of the 31 ^{239}Pu urinary excretions versus the IRFs. Attachment C contains an extended description.

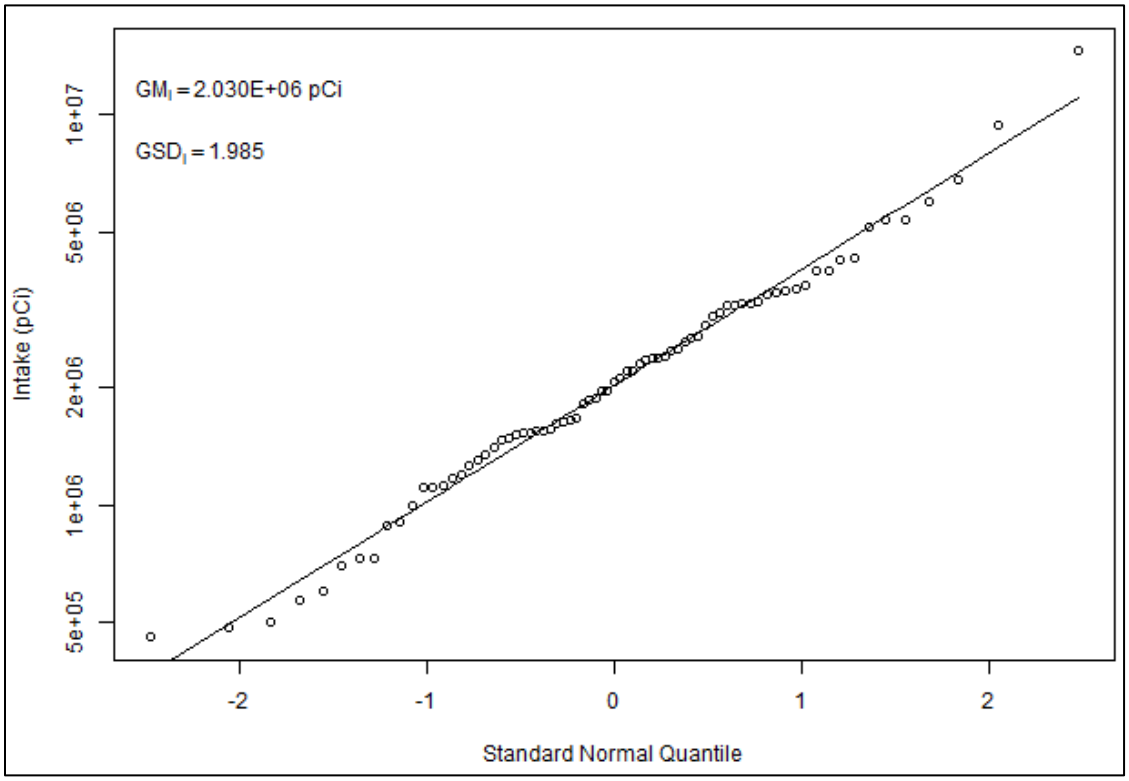

Figure 3-13. Lognormal probability plot of the individual intake estimates from 75 urine bioassays collected after an acute inhalation intake of enriched uranium at Y-12 Plant. Attachment C contains an extended description.

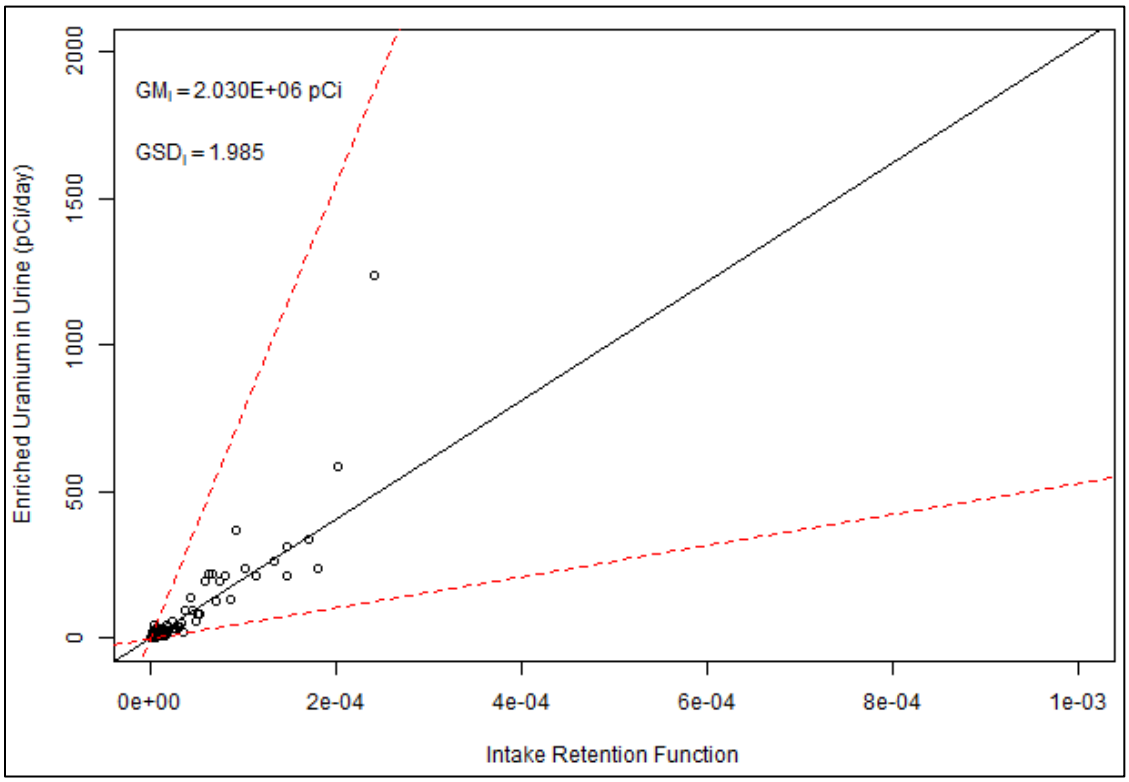

Figure 3-14. Scatterplot of the 75 enriched uranium urinary excretions versus the IRFs. Attachment C contains an extended description.

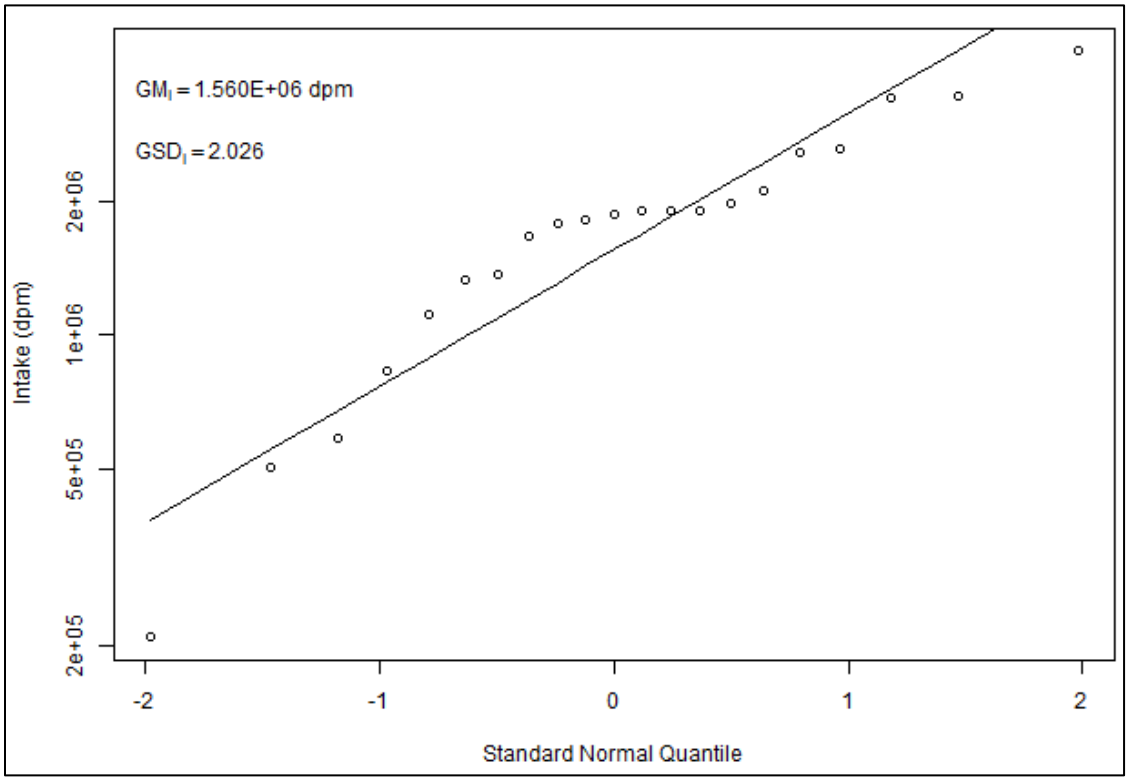

Figure 3-15. Lognormal probability plot of the individual intake estimates from 21 urine bioassays collected after an acute inhalation intake of Type M ^{239}Pu at Rocky Flats Plant. Attachment C contains an extended description.

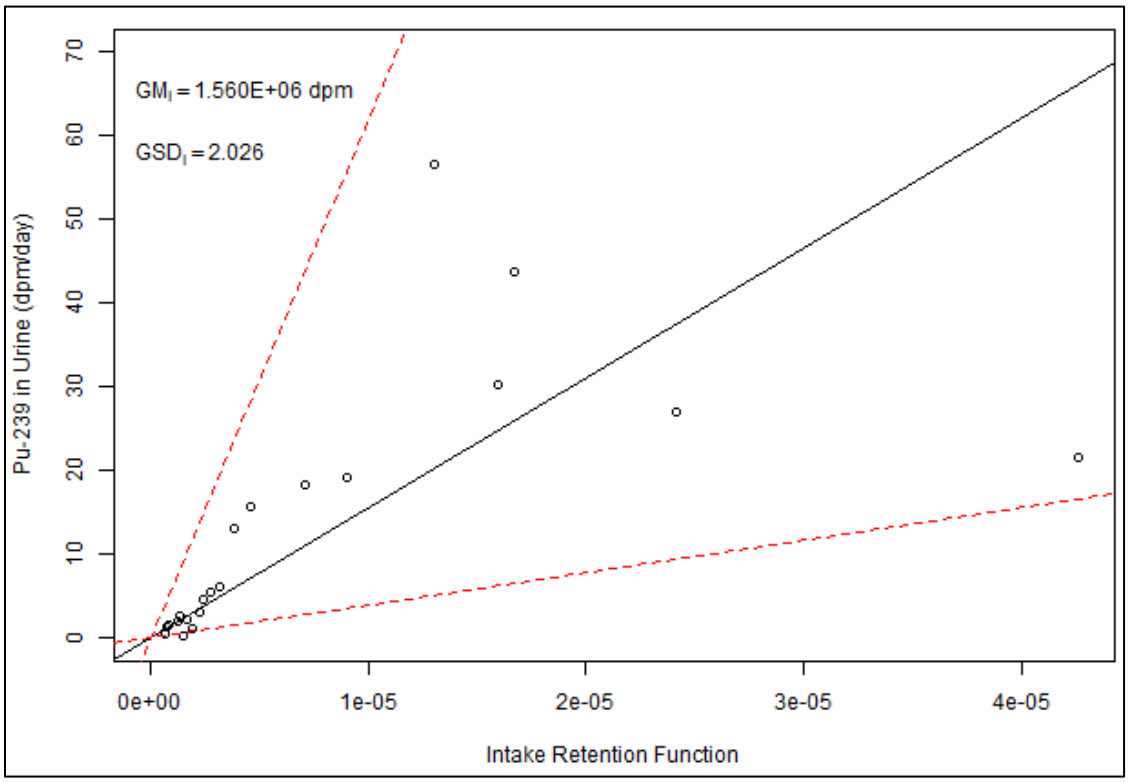

Figure 3-16. Scatterplot of the 21 ^{239}Pu urinary excretions versus the IRFs. Attachment C contains an extended description.

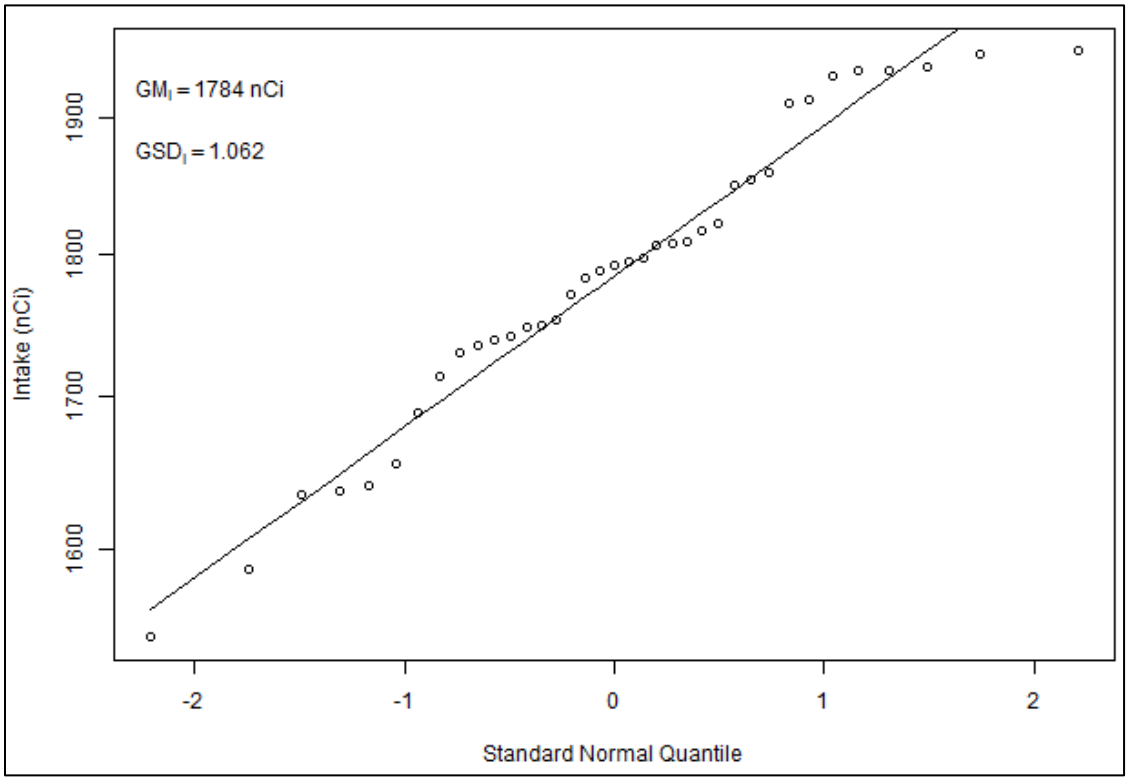

Figure 3-17. Lognormal probability plot of the individual intake estimates from 37 thyroid counts performed after an acute inhalation intake of ^{125}I at a commercial radiopharmaceutical company. Attachment C contains an extended description.

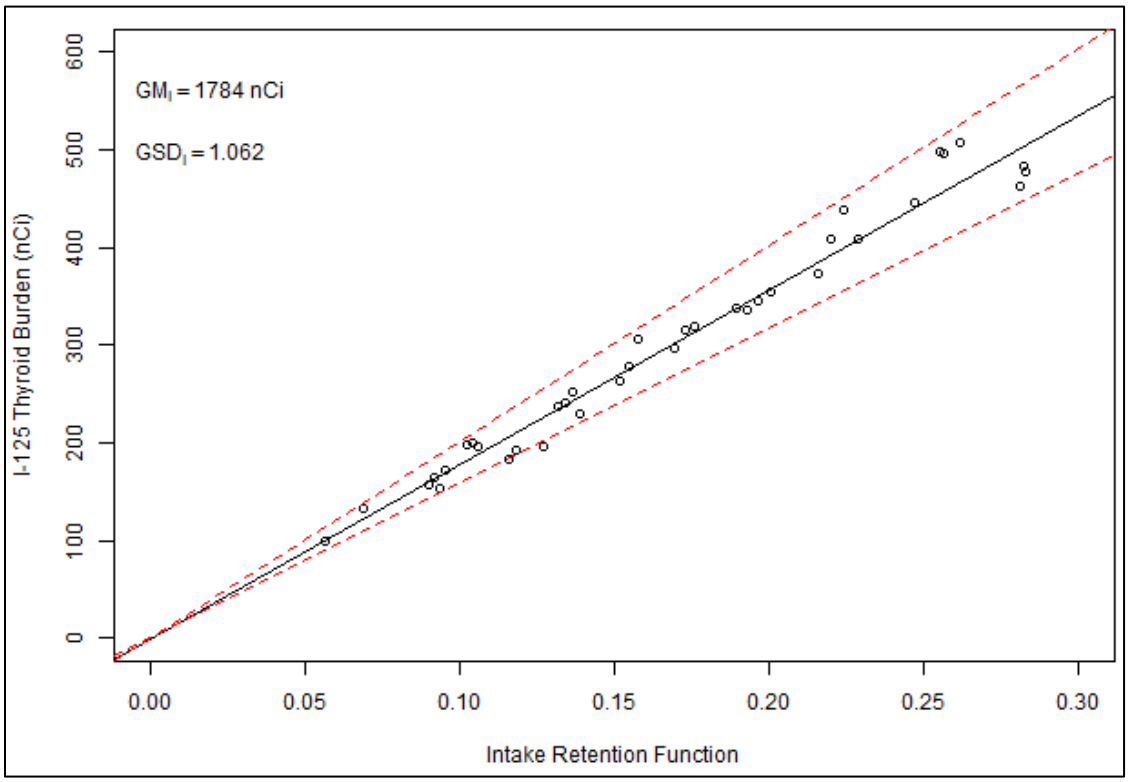

Figure 3-18. Scatterplot of the 37 ^{125}I thyroid burdens versus the IRFs. Attachment C contains an extended description.

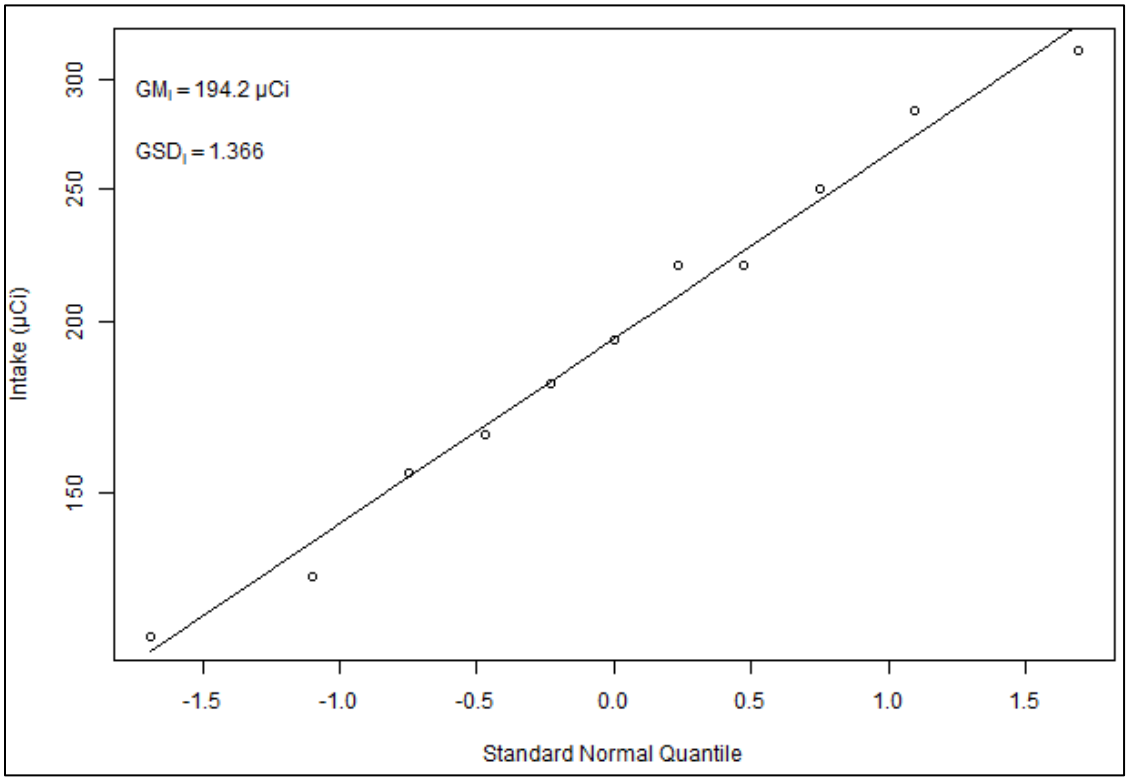

Figure 3-19. Lognormal probability plot of the individual intake estimates from 11 urine bioassays collected after an acute inhalation intake of ^{35}S at a university research reactor. Attachment C contains an extended description.

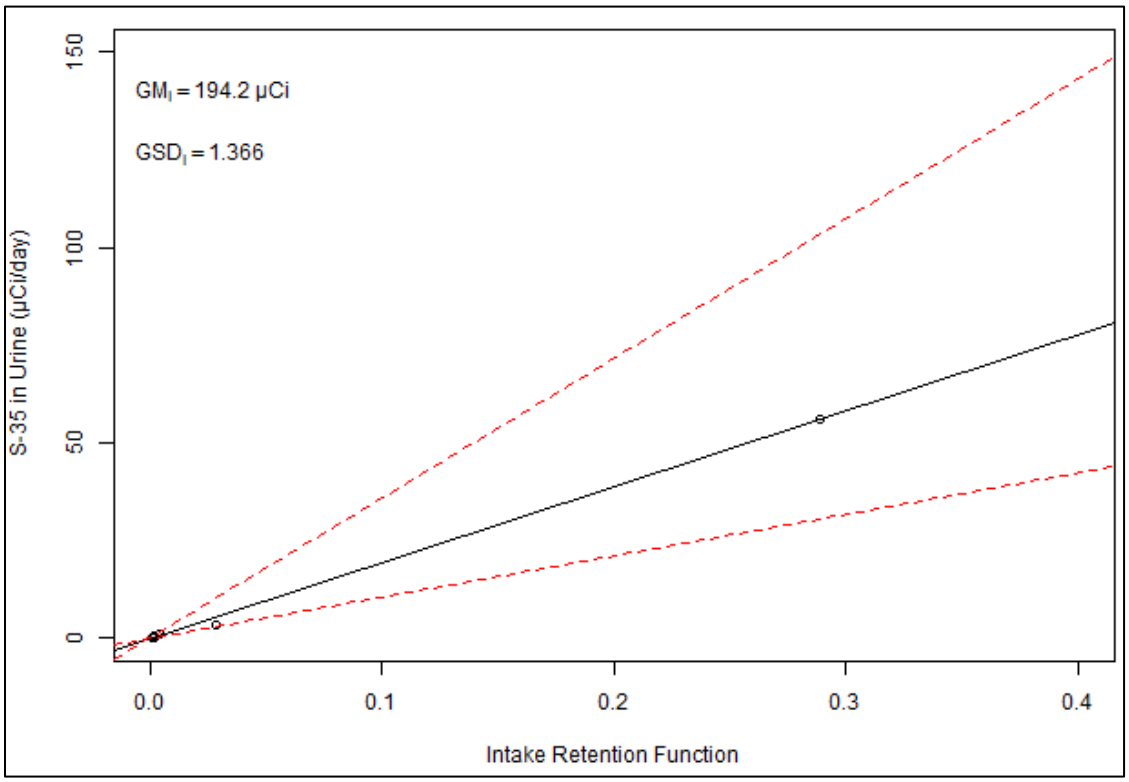

Figure 3-20. Scatterplot of the 11 ^{35}S urinary excretions versus the IRFs. Attachment C contains an extended description.

4.0 UNCERTAINTY IN FITTED DOSE

The uncertainty in the DCFs (fourth column of Table 2-1) must be propagated with the uncertainty in the fitted intakes (Section 3.1 plots) to derive the fitted dose distributions to enter in IREP. The total uncertainty GSD_H in the committed organ dose is:

$$GSD_H = \exp\left[\sqrt{\left(\log GSD_I\right)^2 + \left(\log GSD_{DCF}\right)^2}\right] \quad (4\text{-}1)$$

where

GSD_I = GSD of n intakes
GSD_{DCF} = GSD of DCF

which is shown for each Section 3.1 example in Table 4-1. To be conservative, the values in the GSD_{DCF} column of Table 4-1 are the upper bounds of the ranges from Table 2-1, except for DCF Category E. The largest finite range in the Definition column of Table 2-1 is 85, for Category D. Assume that the category E range is three times as large (255) as the Category D range, resulting in a Category E Definition upper bound of 405. Using an upper bound of 405 and equations (2-2) and (2-6), the GSD_{DCF} for Category E is 2.717.

Table 4-1. Summary of GSD_I calculated for fitted intakes, upper bound of GSD_{DCF} range from Table 2-1, and the propagated GSD_H of the fitted dose.

Nuclide	Pathway	Bioassay	DCF category	GSD_I	GSD_{DCF}	GSD_H
HTO	Inhalation	Urine	A	1.107	1.570	1.588
Cs-137	Inhalation	Whole body count	A	1.216	1.570	1.635
Am-241	Inhalation	Chest count	B	1.099	1.808	1.822
Ce-144	Inhalation	Whole body count	B	1.138	1.808	1.833
Mo-99	Inhalation	Whole body count	C	1.304	2.004	2.105
Pu-239	Wound	Urine	C[a]	1.962	2.004	2.633
U-234	Inhalation	Urine	C	1.985	2.004	2.655
Pu-239	Inhalation	Urine	C	2.026	2.004	2.693
I-125	Inhalation	Thyroid count	D	1.062	2.303	2.308
S-35	Inhalation	Urine	E	1.366	2.717	2.849

a. The category for a wound was assumed to be the same as the category for a Type M inhalation.

5.0 SUMMARY AND CONCLUSIONS

Calculating the uncertainty in doses entered into IREP for dose reconstruction is a complex problem that was simplified by decomposing that uncertainty into the uncertainty in the DCFs and the uncertainty in the fitted intakes.

Pawel et al. [2007] performed an extensive uncertainty analysis on the cancer risk coefficients in FGR-13. Their analysis provided the information used in Section 2.1 to decompose the uncertainty in the cancer risks into the uncertainty in the cancer model and the uncertainty in the DCFs in Table 2-1 as GSD_{DCF} for five categories of radionuclides. These results were corroborated with GSDs derived from 12 cases in NCRP Report No. 164. While the focus of this report is fitted dose, the uncertainties in DCFs in Table 2-1 are applicable for any dose calculations using these DCFs.

The uncertainties in a variety of fitted intakes, represented by GSD_I in Table 4-1, were calculated in Section 3.1. GSD_I and GSD_{DCF} were propagated in Section 4.0, with total uncertainty in fitted dose (GSD_H in Table 4-1) ranging from approximately 1.59 to 2.85. An intake that is intentionally biased has a smaller uncertainty than that of a fitted intake (Attachment B), and the DCF uncertainties in Table 4-1 are the conservative upper bounds of their respective ranges, so the values of GSD_H in Table 4-1

are bounding for dose reconstruction. The fitted dose GSDs, for the variety of examples presented here, are all less than 3. Therefore, for fitted dose, it is acceptable to use a GSD of 3 as the dispersion parameter for a lognormal distribution in IREP.

REFERENCES

Brackett EM, Allen DE, Siebert SR, La Bone TR [2008]. Internal dose reconstruction under part B of the energy employees compensation act. Health Phys *95*(1):69–80. [SRDB Ref ID: 202117]

Boecker B, Hall R, Inn K, Lawrence L, Ziemer P, Eisele G, Wachholzf B, Bun W [1991]. Current status of bioassay procedures to detect and quantify previous exposures to radioactive materials. Health Phys *60*(Suppl. 1):45–100. [SRDB Ref ID: 79440]

Dunning DE Jr., Schwarz G [1981]. Variability of human thyroid characteristics and estimates of dose from ingested I-131. Health Phys *40*(5):661–675. [SRDB Ref ID: 201220]

Eckerman KF, Leggett RW, Cristy M, Nelson CB, Ryman JC, Sjoreen AL, Ward RC [2006]. User's guide to the DCAL system. Oak Ridge National Laboratory, Oak Ridge, TN: UT-Battelle. ORNL/TM-2001/190, August. [SRDB Ref ID: 43944]

Eckerman KF, Leggett RW, Nelson CB, Puskin JS, Richardson ACB [1999]. Cancer risk coefficients for environmental exposure to radionuclides. Washington, DC: U.S. Environmental Protection Agency, Office of Radiation and Indoor Air. Federal Guidance Report 13, September. [SRDB Ref ID: 13719]

Hastie T, Tibshirani R, Friedman J [2008]. The elements of statistical learning data mining, inference, and prediction. 2nd ed. New York: Springer. August. [SRDB Ref ID: 201218]

ICRP [1979a]. ICRP 30 Part 1 - Limits for intakes of radionuclides by workers. ICRP Publication 30 Part 1. Ann ICRP *2*(3/4). [SRDB Ref ID: 29220]

ICRP [1979b]. ICRP 30 Supplement to Part 1 - Limits for intakes of radionuclides by workers. ICRP Publication 30 supplement to Part 1. Ann ICRP *3*(1–4). [SRDB Ref ID: 201219]

ICRP [1981]. ICRP 30 Part 3 - Limits for intakes of radionuclides by workers. ICRP Publication 30 Part 3. Ann ICRP *6*(2/3). [SRDB Ref ID: 168285]

ICRP [1995]. ICRP 68 - Dose coefficients for intakes of radionuclides by workers. ICRP Publication 68. Ann ICRP *24*(4). [SRDB Ref ID: 22731]

NCRP [2009]. NCRP 164 - Uncertainties in internal radiation dose assessment. Bethesda, MD: National Council on Radiation Protection and Measurements. NCRP Report No. 164, July 20. [SRDB Ref ID: 183179]

ORAUT [2018]. Internal dose reconstruction. Oak Ridge, TN: Oak Ridge Associated Universities Team. ORAUT-OTIB-0060 Rev. 02, April 20. [SRDB Ref ID: 171554]

ORAUT [2024]. ORAUT-RPRT-0109 support files. Zip file. Oak Ridge, TN: Oak Ridge Associated Universities Team. February 21. [SRDB Ref ID: 200134]

Pawel DJ, Leggett RW, Eckerman KF, Nelson CB [2007]. Uncertainties in cancer risk coefficients for environmental exposure to radionuclides. Oak Ridge National Laboratory, Oak Ridge, TN: UT-Battelle. ORNL/TM-2006/583, January. [SRDB Ref ID: 200131]

Skrable K, French C, Chabot G, Tries M, La Bone T [2002]. Variance models for estimating intakes from repetitive bioassay measurements. In: Bolch WE, ed. Practical applications of internal dosimetry. Madison, WI: Medical Physics Publishing. [SRDB Ref ID: 201221]

Weisberg S [2005]. Applied linear regression. 3rd ed. Hoboken, NJ: John Wiley & Sons. [SRDB Ref ID: 169440]

ATTACHMENT A
UNCERTAINTY IN ESTIMATED INTAKE

TABLE OF CONTENTS

LIST OF FIGURES

ATTACHMENT A
UNCERTAINTY IN ESTIMATED INTAKE (continued)

A.1 INTRODUCTION

This attachment demonstrates a weighted least squares regression of bioassay data on IRFs to estimate intakes and their uncertainties.

A.2 BIOASSAY DATA

The bioassay data for this example consist of 37 thyroid counts *M* over approximately 90 days performed at times *t* on an individual with an acute injection intake of ^{125}I. The ICRP Publication 68 [ICRP 1995] IRFs *m* were calculated with DCAL [Eckerman et al. 2006]. A scatterplot of the thyroid counts versus the IRFs is shown in Figure A-1.

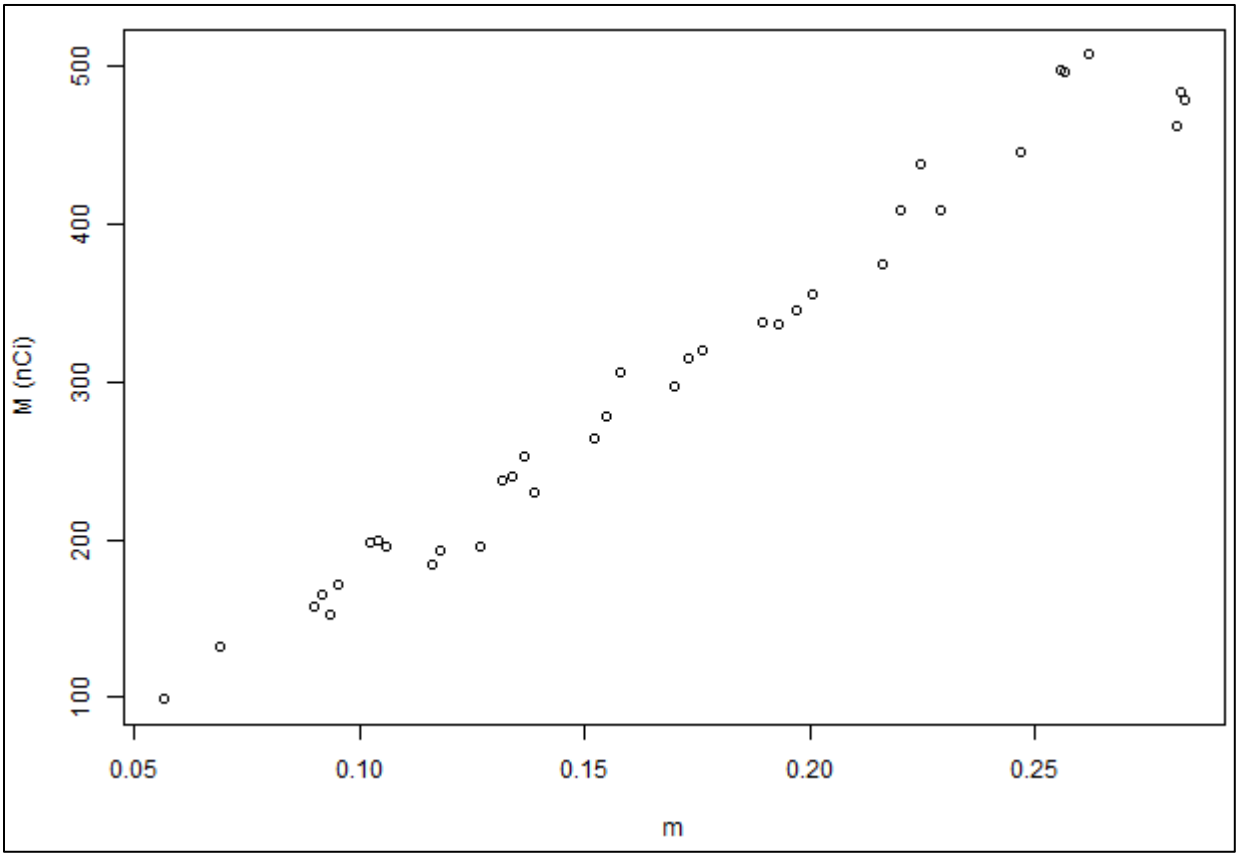

Figure A-1. Scatterplot of thyroid counts (*M*) versus IRFs (*m*).

A.3 LEAST SQUARES REGRESSION

By the definition of an IRF, an intake I_i can be calculated from a single bioassay result and its associated IRF, which are both a function of time:

$$I_i = \frac{M(t_i)}{m(t_i)} \tag{A-1}$$

ATTACHMENT A
UNCERTAINTY IN ESTIMATED INTAKE (continued)

Multiple bioassay measurements are typically evaluated by treating the relationship between the bioassay data and IRFs as a straight line through the origin with the intake *I* being the slope of the line:

$$M(t_i) = Im(t_i) + \varepsilon(t_i) \quad (i = 1, 2, \ldots, n) \tag{A-2}$$

where

n = number of bioassay measurements
t_i = time of the ith thyroid count
$\varepsilon(t_i)$ = error at time t_i

The expression in Equation A-2 can be simplified by applying indices to the bioassay data and IRFs to suppress the time argument:

$$M_i = Im_i + \varepsilon_i \tag{A-3}$$

This relationship can be expressed in standard statistical notation, with the response variable *Y* being the bioassay data *M*, the predictor variable *X* being the IRFs *m*, and the intake *I* being the slope β:

$$Y_i = \beta X_i + \varepsilon_i \tag{A-4}$$

In all practical applications the population mean is unknown and unknowable, so the error is unknown and unknowable.[7] Because there are portions of Equation A-4 that are unknown and unknowable, instead of dealing with the formal relationship in Equation A-4, the fitted relationship must be considered:

$$E(Y_i) = \hat{Y}_i = BX_i \tag{A-5}$$

where

$E(Y_i)$ = expectation of Y_i
$\hat{Y}_i$ = predicted value of Y_i
B = estimate of the true intake β

Population parameters like the slope β are represented with Greek letters. Sample statistics like the slope *B* are represented with italic letters and are calculated with the observed data. If *B* is an unbiased estimator, its expectation is equal to β. The residuals r_i are defined as:

$$r_i = Y_i - BX_i = Y_i - \hat{Y}_i \tag{A-6}$$

Although the residuals are not the errors, they contain all the empirical information about the errors.

---

7 If the population mean was known, this discussion would not be necessary.

ATTACHMENT A
UNCERTAINTY IN ESTIMATED INTAKE (continued)

The task of estimating the intake from the bioassay data as described is a regression through the origin, which is amongst the simplest of all regression models [Weisberg 2005, pp. 56–57]. In a perfect fit of a statistical model to a set of data, each of the residuals as defined in Equation A-6 would equal zero. Therefore, it makes sense to define a good fit as one that makes the residuals, or some function of the residuals, as close to zero as possible for a given set of data. Various functions of the residuals can be used, but of greatest historical and practical significance is choosing a fit to minimize the sum of the squares of the residuals (least squares fit) [Weisberg 2005, p. 287]. Therefore, the sum of squares *SS* is:

$$SS = \sum_{i=1}^{n} r_i^2 = \sum_{i=1}^{n} \left(Y_i - BX_i\right)^2 \tag{A-7}$$

To minimize the sums of squares, differentiate it with respect to *B*, set the result equal to zero, and solve for *B,* which gives:

$$B = \frac{\sum_{i=1}^{n} Y_i X_i}{\sum_{i=1}^{n} X_i^2} \tag{A-8}$$

This is referred to as the least squares solution for regression through the origin.

A.4 WEIGHTED LEAST SQUARES REGRESSION

Least squares regression assumes identical uncertainties in all bioassay results (homoscedasticity). If the uncertainties are different (heteroscedasticity), as they almost always are with bioassay data, a weighted least squares regression should be performed [Weisberg 2005, pp. 110–112]:

$$B_w = \frac{\sum_{i=1}^{n} w_i Y_i X_i}{\sum_{i=1}^{n} w_i X_i^2} \tag{A-9}$$

where the weights *w* are the inverse of the variances (σ^2) of the data:

$$w_i = \frac{1}{\sigma_i^2} \tag{A-10}$$

Skrable et al. [2002] discuss different ways of specifying the variances, including the slopes method, where the variance is proportional to the square of the IRF:

$$\sigma_i^2 = kX_i^2 \tag{A-11}$$

Note that *k* is a proportionality constant that does not influence the estimated intake or its standard error, so assume $k = 1$.

ATTACHMENT A
UNCERTAINTY IN ESTIMATED INTAKE (continued)

Substituting for w_i in the right-hand side of Equation A-9 using Equations A-10 and A-11 and simplifying gives:

$$B_w = \frac{1}{n}\sum_{i=1}^{n}\frac{Y_i}{X_i} = \frac{1}{n}\sum_{i=1}^{n} b_i \qquad \text{(A-12)}$$

where b_i is the intake calculated from bioassay result Y_i as mentioned in Equation A-1. In essence, the slopes method gives the mean of the n intakes (slopes) calculated from the n bioassay results, which is shown in Figure A-2. The pink lines in Figure A-2 are lines going through the origin and each of the 37 thyroid counts; the slope of the black line is the arithmetic mean (Equation A-12) of the slopes of those 37 lines.

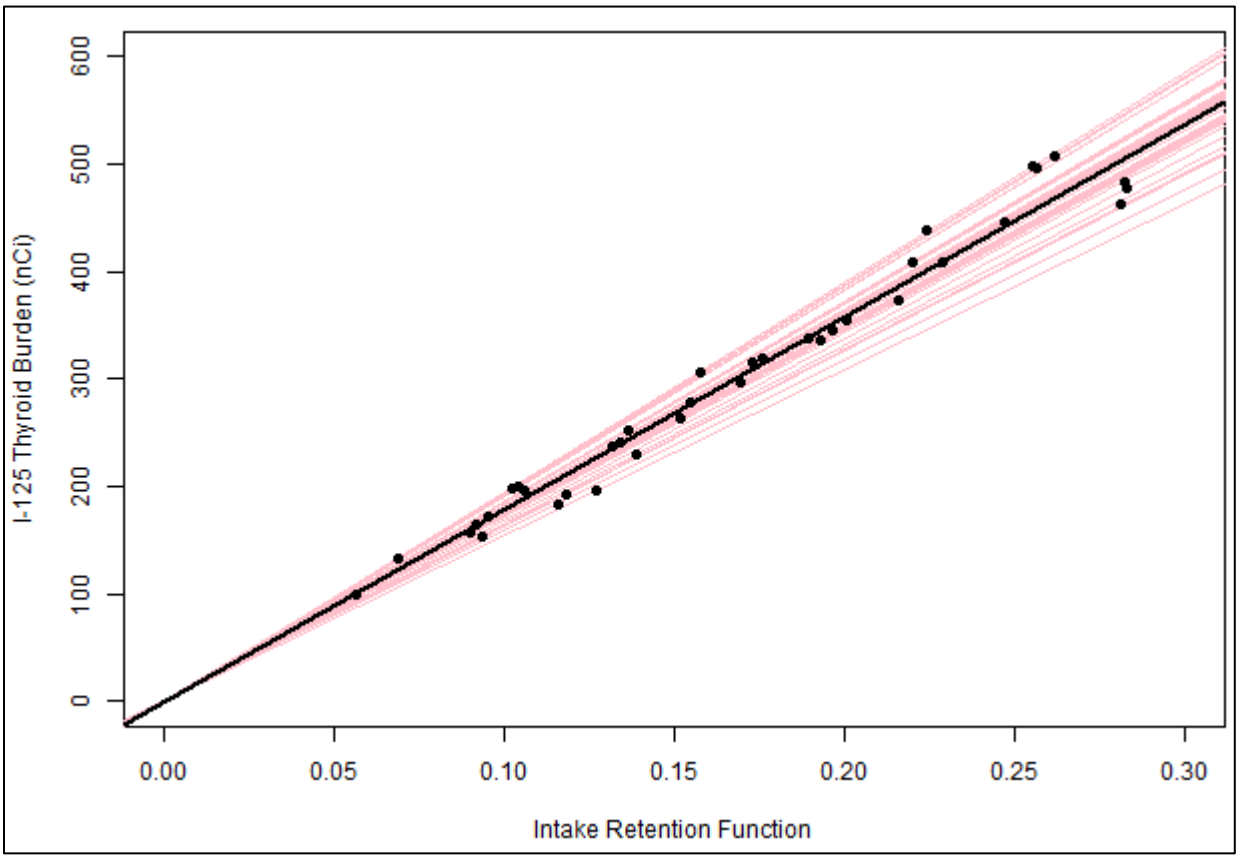

Figure A-2. Scatterplot of thyroid burdens versus IRFs. The narrow pink lines are lines going through each of the thyroid counts and the origin. The slope of the wide black line is the mean of the slopes of the narrow pink lines. Attachment C contains an extended description.

The variance of the individual intakes b_i around the mean intake B_w is:

$$\sigma^2 = \frac{1}{n-1}\sum_{i=1}^{n}\left(b_i - B_w\right)^2 \qquad \text{(A-13)}$$

The arithmetic mean and variance, in Equations A-12 and A-13 respectively, imply a normal distribution. Some advantages of using a lognormal distribution over the normal distribution are:

ATTACHMENT A
UNCERTAINTY IN ESTIMATED INTAKE (continued)

(1) the uncertainty in the intake represented by the GSD is restricted to positive real values, (2) the uncertainty in the intake can be easily propagated with the uncertainty in the DCF because they are both lognormal, and (3) the GM is more resistant to outliers than the arithmetic mean.

The sample GM B_g of the n intakes is:

$$B_g = \exp\left(\frac{1}{n}\sum_{i=1}^{n}\log(b_i)\right) \quad \text{(A-14)}$$

and the sample GSD σ_g is a measure of dispersion of b_i around B_g:

$$\sigma_g = \exp\left[\sqrt{\frac{1}{n-1}\sum_{i=1}^{n}\left(\log(b_i)-\log(B_g)\right)^2}\right] \quad \text{(A-15)}$$

The lognormal probability plot in Figure A-3 shows that a lognormal distribution with parameters $\log(B_g)$ and $\log(\sigma_g)$ fits the intakes very well.

Note that in the body of this report GM_l is used instead of B_g and GSD_l is used instead of σ_g to be consistent with the standard notation used in project documents.

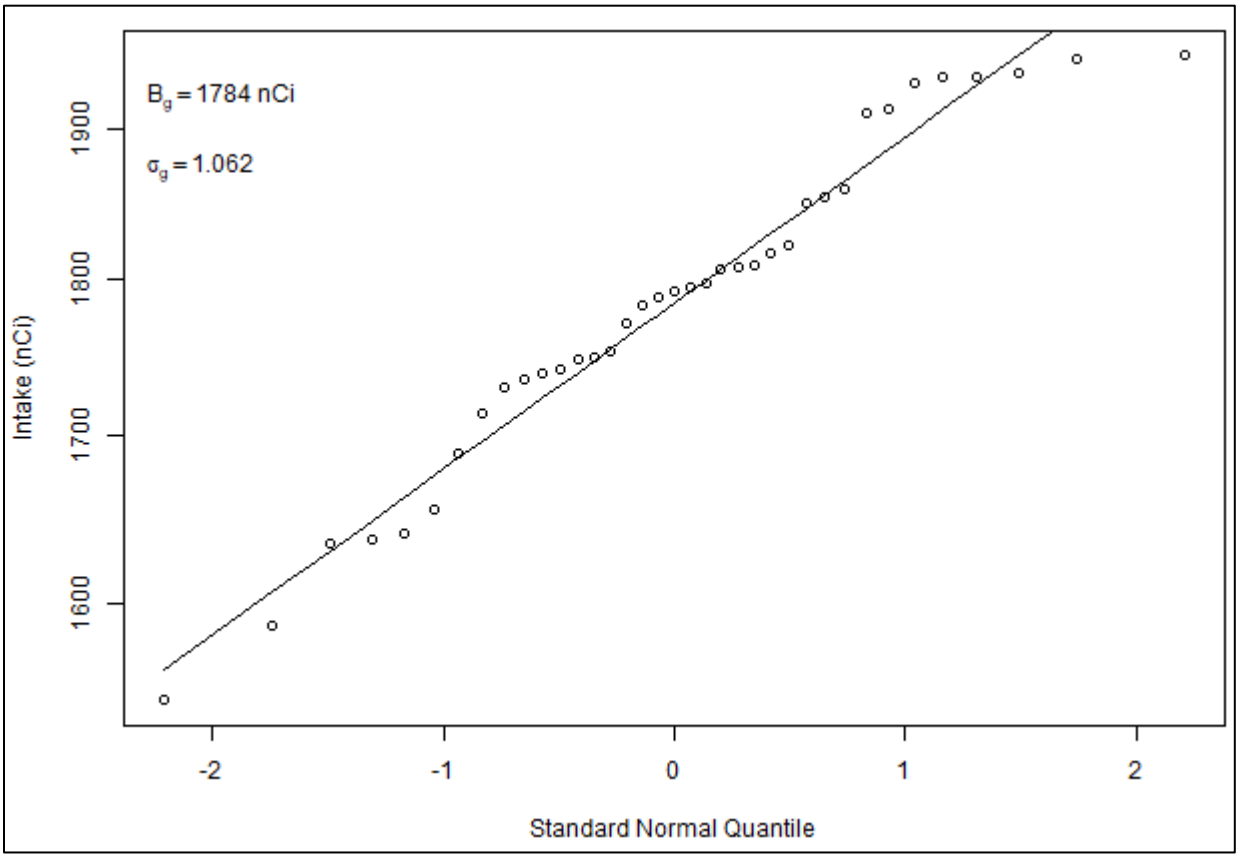

Figure A-3. Lognormal probability plot of the individual intake estimates (same as Figure 3-17 except for the notation for the summary statistics). Attachment C contains an extended description.

ATTACHMENT A
UNCERTAINTY IN ESTIMATED INTAKE (continued)

The GM intake B_g (black line) and the 95% prediction interval for individual intakes (dashed red lines) are shown in Figure A-4.

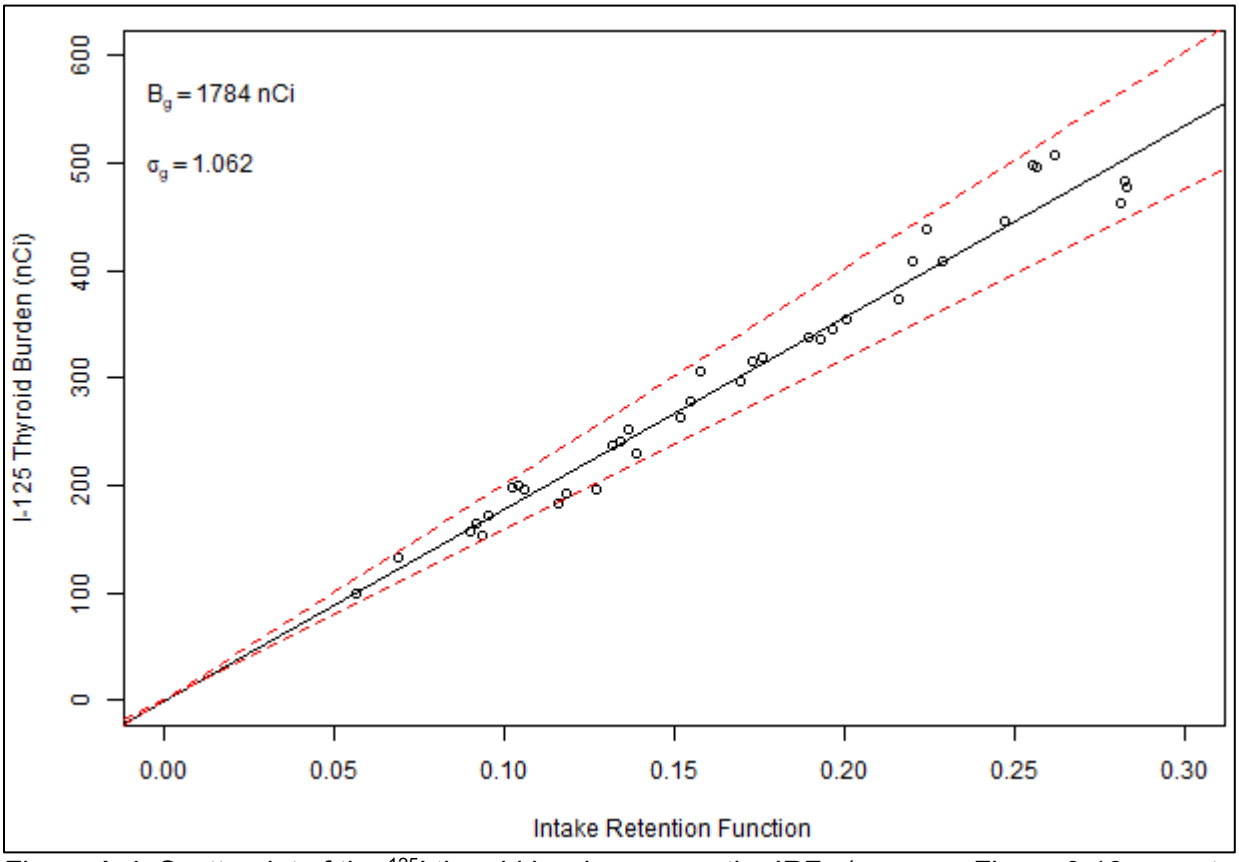

Figure A-4. Scatterplot of the ^{125}I thyroid burden versus the IRFs (same as Figure 3-18 except for the notation for the summary statistics). Attachment C contains an extended description.

ATTACHMENT B
BIAS-VARIANCE TRADEOFF

TABLE OF CONTENTS

LIST OF TABLES

LIST OF FIGURES

ATTACHMENT B
BIAS-VARIANCE TRADEOFF (continued)

B.1 INTRODUCTION

As discussed in Attachment A, weighted least squares regression of bioassay data on IRFs is a best estimate of fitted intakes. This attachment demonstrates that an intake that has been intentionally biased (high or low) has a smaller uncertainty than the uncertainty in a best-estimate fitted intake.

B.2 EXAMPLE

The ICRP Publication 30 biokinetic model for iodine is shown in Figure B-1 [ICRP 1979a, p. 51]. The rate constants for the model are in Table B-1. The natural variability in these rate constants was not addressed by ICRP, but Dunning and Schwarz [1981, p. 10] described the retention times of iodine in the adult thyroid with a lognormal distribution having a GM of 72 days and a GSD of 1.76. To calculate the rate constants for the thyroid, the GM of the distribution is the Publication 30 value of 80 days [ICRP 1981, p. 134] for the biological half-life of iodine in the thyroid, and the GSD is 1.76 from Dunning and Schwarz [1981, p. 10]. The rate constants for the other compartments are calculated from GMs equal to their respective Publication 30 half-life and a GSD equal to 1.5.[8] Note that the rate constants are assumed to be uncorrelated, which is most likely not correct. However, this assumption is necessary because essentially no information about correlations of the rate constants is available in the literature.

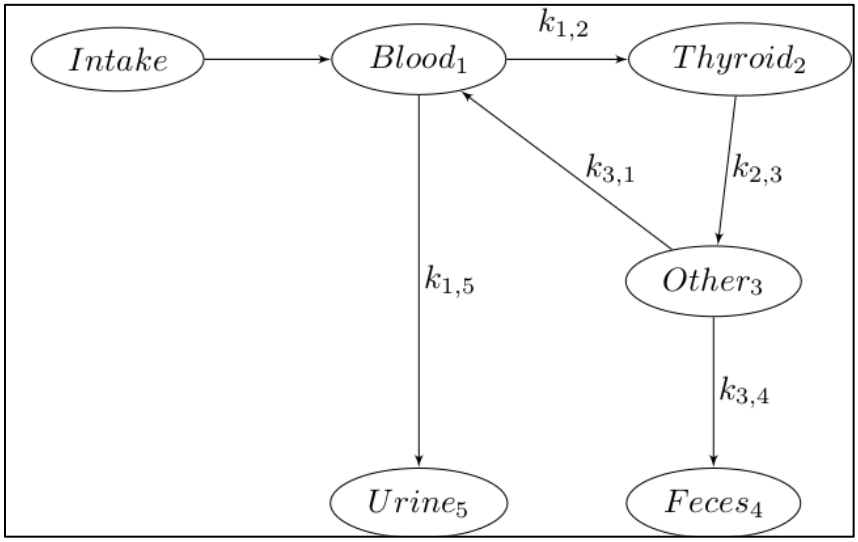

Figure B-1. Riggs iodine compartmental model. Attachment C contains an extended description.

[8] The relationship between the biased and unbiased distributions has been observed to be the same for GSD values in the range of 1.5 to 3.

ATTACHMENT B
BIAS-VARIANCE TRADEOFF (continued)

Table B-1. Rate constants for ICRP Publication 30 iodine model. Rate constants on the diagonal of the rate matrix (e.g., $k_{2,2}$) are the sum of all rate constants for material leaving that compartment [ICRP 1979a, p. 51].[a]

From	To	Rate constant (1/d)	Half life (d)
blood	thyroid	$k_{1,2}$ = 0.8318	N/A
blood	urine	$k_{1,5}$ = 1.941	N/A
other	feces	$k_{3,4}$ = 0.005776	N/A
other	blood	$k_{3,1}$ = 0.05199	N/A
thyroid	other	$k_{2,3}$ = 0.008664	N/A
other	N/A	$k_{3,3}$ = 0.05777	12
blood	N/A	$k_{1,1}$ = 2.773	0.25
urine	N/A	$k_{5,5}$ = 0	∞
feces	N/A	$k_{4,4}$ = 0	∞
thyroid	N/A	$k_{2,2}$ = 0.008664	80

a. N/A = not applicable.

For this exercise, first calculate an unbiased interval estimate of the committed dose to the thyroid resulting from a 1 Bq uptake of elemental ^{125}I:

1. Draw random values for the rate constants from their respective lognormal distributions and calculate the number of transformations in the thyroid.

2. Repeat the simulation 50,000 times to obtain a distribution of transformations.

3. Convert the transformations to thyroid dose.[9]

Then calculate a biased-high estimate of the number of transformations, by fixing the $k_{2,3}$ rate constant for the thyroid at the 5th percentile of its lognormal distribution (which gives the same result as fixing the thyroid half-life at its 95th percentile, 204 days) and repeating simulation steps 1 through 3. The resulting distributions for biased and unbiased estimates are shown in Figure B-2.

9 Using 1.4 × 10^{-3} MeV/g to the thyroid per transformation [ICRP 1979b, p. 201]

ATTACHMENT B
BIAS-VARIANCE TRADEOFF (continued)

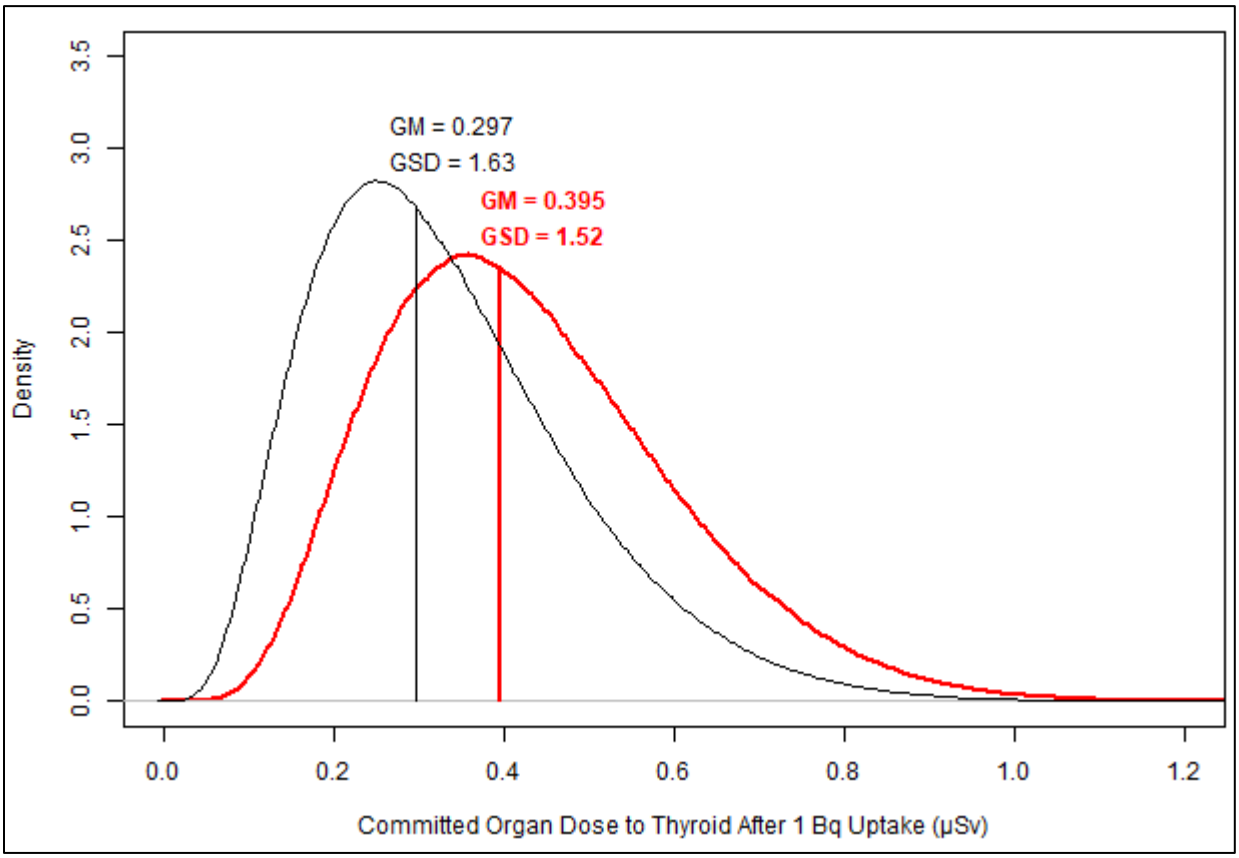

Figure B-2. Density plot of the committed dose to the thyroid after a 1 Bq uptake of ^{125}I. The black curve is the unbiased estimate, and the bold red curve is the biased estimate. An empirical GM and GSD are given for each distribution. Attachment C contains an extended description.

B.3 CONCLUSION

If the objective is to calculate the most accurate estimate of the thyroid dose given the uncertainty in the rate constants, an uncertainty analysis like the one shown above for the unbiased case is appropriate. When replacing the uncertainty in the thyroid rate constant with a conservative constant, the resulting distribution is biased high[10] and variability is removed, as reflected in the higher GM and smaller GSD. Taken to the extreme case, if all rate constants are set to conservative constants the result of the deterministic calculation is a biased high point estimate with no uncertainty. The general idea is that every time an unbiased estimate is replaced with a conservative nonstochastic value, the result is biased high (intended) and its uncertainty is reduced (perhaps not expected). A related phenomenon in machine learning and statistics is referred to as the bias-variance tradeoff, where introducing bias reduces the variance and lowers the overall uncertainty of the calculated quantity [Hastie et al. 2008, pp. 57–58].

In this application, the bias-variance tradeoff implies that the uncertainty in best estimates of intake or dose is larger than the uncertainty from the biased estimates. In addition, the uncertainty in an

[10] Note that if the estimate is biased low by using the 5th percentile of the thyroid half-life, then both the GM and GSD are reduced.

ATTACHMENT B
BIAS-VARIANCE TRADEOFF (continued)

unbiased estimate is larger than the uncertainty in a biased estimate because the two uncertainties mean different things:

- For an unbiased estimate, the probability that the true value is within a stated interval around the estimated value; and

- For an estimate that is biased high, the probability that the true value is larger than the estimate, which tends to be quite small by design.

ATTACHMENT C
EXTENDED DESCRIPTIONS OF FIGURES

Figure 2-2
Probability plot of organ dose GSDs with x-axis “Standard Normal Quantiles” from ranges from -2 to 2 and y-axis “GSD of Estimated Dose” from 1 to 3.5. Horizontal dot-dashed line at GSD = 3. Loosely diagonal pattern of dots goes from bottom left to upper right with straight line through them.

Figure 3-1
Probability plot with x-axis “Standard Normal Quantile” from about -2 to 2 and log-scaled y-axis “Intake (µCi)” from about 1800 to 3200. Fairly linear pattern of 29 dots go from the bottom left to the middle right side with straight line. There is an additional point at approximately (1, 3200). Text says, “GM sub i equals 2175 µCi and GSD sub i equals 1.107.”

Figure 3-2
Scatterplot with x-axis “Intake Retention Function” from 0 to 1 and y-axis “HTO Body Burden (µCi) from 0 to 2500. Fairly linear pattern of 29 dots from about (0, 0) to (0.85, 2000). Black line goes from (0, 0) to about (1, 2200). Two red lines start at (0, 0); one goes to about (1, 1700) and other to about (0.95, 2500). Text says, “GM sub i equals 2175 µCi and GSD sub i equals 1.107.”

Figure 3-3
Probability plot with x-axis “Standard Normal Quantile” from about -1.5 to 1.5 and log-scaled y-axis “Intake (MBq)” from about 0.07 to 0.13. Fairly linear pattern of 7 dots from bottom left to middle right side. Straight line runs through the dots. Text says, “GM sub i equals 0.1084 MBq and GSD sub i equals 1.216.”

Figure 3-4
Scatterplot with x-axis “Intake Retention Function” from 0 to 0.7 and y-axis “Cs-137 Body Burden (MBq)” from 0 to 0.1. Fairly linear pattern of 7 dots from about (0, 0) to (0.65, 0.07). Black line goes from (0, 0) to about (0.7, 0.8). Two red lines start at (0, 0); one goes to about (0.7, 0.05) and other to about (0.65, 0.1). Text says, “GM sub i equals 0.1084 MBq and GSD sub i equals 1.216.”

Figure 3-5
Probability plot with x-axis “Standard Normal Quantile” from about -2 to 2 and log-scaled y-axis “Intake (Bq)” from about 160 to 230. Fairly linear pattern of 16 dots from bottom left to top right. Straight line runs through the dots. Text says, “GM sub i equals 199.4 Bq and GSD sub i equals 1.099.”

Figure 3-6
Scatterplot with x-axis “Intake Retention Function” from 0 to 0.15 and y-axis “Am-241 Chest Burden (Bq)” from 0 to 30. Cloud pattern of 16 dots from about (0.08, 17) to (0.12, 27). Black line goes from (0, 0) to about (0.15, 30). Two red lines start at (0, 0); one goes to about (0.15, 25) and other to about (0.13, 30). Text says, “GM sub i equals 199.4 Bq and GSD sub i equals 1.099.”

Figure 3-7
Probability plot with x-axis “Standard Normal Quantile” from about -1.5 to 1.5 and log-scaled y-axis “Intake (µCi)” from about 1200 to 1800. Fairly linear pattern of 6 dots from bottom left to top right corner. Straight line runs through the dots. Text says, “GM sub i equals 1502 nCi and GSD sub i equals 1.138.”

Figure 3-8
Scatterplot with x-axis “Intake Retention Function” from 0 to 0.065 and y-axis “Ce-144 Body Burden (nCi)” from 0 to 150. Fairly linear pattern of 6 dots goes from about (0.02, 30) to (0.062, 100). Black

ATTACHMENT C
EXTENDED DESCRIPTIONS OF FIGURES (continued)

line goes from (0, 0) to about (0.065, 100). Two red lines start at (0, 0); one goes to about (0.065, 70) and the other to about (0.065, 125). Text says, “GM sub i equals 1502 nCi and GSD sub i equals 1.138.”

Figure 3-9
Probability plot with x-axis “Standard Normal Quantile,” from about -1.5 to 1.5 and log-scaled y-axis “Intake (µCi)” from about 15 to 35. Fairly linear pattern of 10 dots goes from bottom left to top right corner. Straight line runs through the dots. Text says, “GM sub i equals 20.98 µCi and GSD sub i equals 1.304.”

Figure 3-10
Scatterplot with x-axis “Intake Retention Function” from 0 to 1 and y-axis “Mo-99 Body Burden (µCi)” from 0 to 20. Fairly linear pattern of 10 dots goes from about (0, 0) to (0.75, 14). Black line goes from (0, 0) to approximately (1, 20). Two red lines start at (0, 0); one goes to about (1, 12) and the other about to (0.55, 20). Text says, “GM sub i equals 20.98 µCi and GSD sub i equals 1.304.”

Figure 3-11
Probability plot with x-axis “Standard Normal Quantile” from about -2 to 2 and log-scaled y-axis “Intake (Bq)” from about 3 to 50. Fairly linear pattern of 31 dots goes from bottom left to top right corner. Straight line runs through the dots. Text says, “GM sub i equals 18.16 Bq and GSD sub i equals 1.962.”

Figure 3-12
Scatterplot with x-axis “Intake Retention Function” from 0 to 0.003 and y-axis “Pu-239 in 24-hour Urine (Bq)” from 0 to 0.05. Of the 31 dots, 27 form a fairly linear pattern from about (0, 0) to (0.0002, 0.01). Four more dots are at about (0.0005, 0.012), (0.0006, 0.018), (0.0015, 0.038), and (0.0026, 0.03). Black line goes from (0, 0) to about (0.0028, 0.05). Two red lines start at (0, 0); one goes to about (0.003, 0.012) and other to about (0.0007, 0.05). Text says, “GM sub i equals 18.16 Bq and GSD sub i equals 1.962.”

Figure 3-13
Probability plot with x-axis “Standard Normal Quantile” from about -2.5 to 2.5 and log-scaled y-axis “Intake (pCi)” from about 5e5 to 5e7. 75 dots go from bottom left to top right corner. Straight line runs through the dots. Text says, “GM sub i equals 2.030e6 pCi and GSD sub i equals 1.985.”

Figure 3-14
Scatterplot with x-axis “Intake Retention Function” from 0 to 1e-3 and y-axis “U-238 in Urine (pCi/day)” from 0 to 2000. All dots but one are linearly related from (0, 0) to (2e-4, 600). The other point is approximately (2.2e4, 1300). Black line goes from (0, 0) to about (1e-3, 2000). Two red lines start at (0, 0); one goes to about (1e-3, 500) and other to about (2.3e-4, 2000). Text says, “GM sub i equals 2.030e6 pCi and GSD sub i equals 1.985.”

Figure 3-15
Probability plot with x-axis is labeled “Standard Normal Quantile” from about -2 to 2 and log-scaled y-axis “Intake (dpm)” from about 2e5 to 5e6. Fairly linear pattern of 21 dots goes from the bottom left corner to the top right corner. Straight line runs through the dots. Text says, “GM sub i equals 1.56e6 dpm and GSD sub i equals 2.026.”

ATTACHMENT C
EXTENDED DESCRIPTIONS OF FIGURES (continued)

Figure 3-16
Scatterplot with x-axis is labeled “Intake Retention Function” from 0 to 4.2e-5 and y-axis “Pu-239 in Urine (dpm/day)” from 0 to 70. Of 21 dots, 16 are in a fairly linear pattern from about (0, 0) to (1e-5, 20). The other 5 dots are approximately (1.2e-5, 55), (1.5e-5, 30), (1.6e-5, 42), (2.3e-5, 25), and (4.2e-5, 20). The black line goes from (0, 0) to about (4.2e-5, 70). Two red dashed lines start at (0,0); one goes to about (4.2e-5, 17) and the other about (1e-5, 70). Text says, “GM sub i equals 1.56e6 dpm and GSD sub i equals 2.026.”

Figure 3-17
Probably plot with x-axis “Standard Normal Quantile” from about -2 to 2 and log-scaled y-axis “Intake (nCi)” from about 1500 to 2000. Fairly linear pattern of 37 dots from bottom left corner to the top right corner. Straight line runs through the dots. Text says, “GM sub i equals 1784 nCi and GSD sub i equals 1.062.”

Figure 3-18
Scatterplot with x-axis is labeled “Intake Retention Function” from 0 to 0.3 and y-axis “I-125 Thyroid Burden (nCi)” from 0 to 600. Fairly linear pattern of 37 dots from about (0.05, 100) to (0.28, 500). Black line goes from (0, 0) to approximately (0.3, 550). Two red dashed lines start at (0, 0); one goes to about (0.3, 475) and other to about (0.3, 600). Text says, “GM sub i equals 1784 nCi and GSD sub i equals 1.062.”

Figure 3-19
Probability plot with x-axis “Standard Normal Quantile” from about -2 to 2 and log-scaled y-axis “Intake (µCi)” from about 100 to 300. Fairly linear pattern of 11 dots from bottom left corner to the top right corner. Straight line runs through the dots. Text says, “GM sub i equals 194.2 µCi and GSD sub i equals 1.366.”

Figure 3-20
Scatterplot with x-axis “Intake Retention Function” from 0 to 0.4 and y-axis “S-35 in Urine (µCi/day)” from 0 to 150. Nine of the 11 dots are near (0, 0). The other two dots are at approximately (0.02, 5) and (0.3, 50). Black line goes from (0, 0) to approximately (0.4, 80). Two red dashed lines start at (0, 0); one goes to about (0.4, 40) and other about (0.4, 150). Text says, “GM sub i equals 194.2 µCi and GSD sub i equals 1.366.”

Figure A-2
Scatterplot with x-axis “Intake Retention Function” from 0 to 0.3 and y-axis “I-125 Thyroid Burden (nCi)” from 0 to 600. Fairly linear pattern of 37 dots goes from about (0.05, 100) to (0.28, 500). Black line goes from (0, 0) to about (0.3, 550). Each of 37 pink lines goes through (0, 0) and one of the 37 dots.

Figure A-3
Probability plot with x-axis “Standard Normal Quantile” from about -2 to 2 and log-scaled y-axis “Intake (nCi), from about 1500 to 2000. Fairly linear pattern of 37 dots goes from bottom left to top right corner. Straight line runs through the dots. Text says, “B sub g equals 1784 nCi and sigma sub g equals 1.062.”

Figure A-4
Scatterplot with x-axis “Intake Retention Function” from 0 to 0.3 and y-axis “I-125 Thyroid Burden (nCi)” from 0 to 600. Fairly linear pattern of 37 dots goes from about (0.05, 100) to (0.28, 500). Black

ATTACHMENT C
EXTENDED DESCRIPTIONS OF FIGURES (continued)

line goes from (0, 0) to about (0.3, 550). Two red lines start at (0, 0); one goes to about (0.3, 475) and other to about (0.3, 600). Text says, “B sub g equals 1784 nCi and sigma sub g equals 1.062.”

Figure B-1
This compartmental model looks like a flowchart. At top left is an oval labeled “Intake.” A horizontal arrow points right from “Intake” to another oval labeled “Blood sub 1.” A vertical arrow labeled “k sub 1,5” points from “Blood sub 1” down to an oval labeled “Urine sub 5” at bottom of the diagram. A horizontal arrow labeled “k sub 1,2” points right from “Blood sub 1” to an oval labeled “Thyroid sub 2.” A vertical arrow labeled “k sub 2,3” points down from “Thyroid sub 2” to an oval labeled “Other sub 3” halfway down the diagram. A diagonal arrow points up and left from “Other sub 3” back to “Blood sub 1.” A vertical arrow labeled “k sub 3,4” points down from “Other sub 3” to an oval labeled “Feces sub 4” at bottom of the diagram.

Figure B-2
Density plot with x-axis “Committed Organ Dose in μSv to Thyroid After 1 Bq Uptake” from 0 to 1.2 and y-axis “Density” from 0 to 3.5. Two lognormal densities are plotted. Black curve apex at about 0.2 with GM as vertical line at 0.297. Most of curve is between x values of 0 and 0.9. Text says, “GM equals 0.297 and GSD equals 1.63.” Red curve apex at about 0.37 with GM as vertical line at 0.395. Most of curve is between x values of 0.07 and 1. Text says, “GM equals 0.395 and GSD equals 1.52.”